CENTRAL RESEARCH LIBRARY
DOCUMENT COLLECTION

MARTIN MARIETTA ENERGY SYSTEMS LIBRARIES
3 4456 0360592 6

ORNL 1283
Instrumentation

9a

GENERAL PRINCIPLES OF A PROTON RECOIL FAST-NEUTRON SPECTROMETER

CENTRAL RESEARCH LIBRARY
DOCUMENT COLLECTION

LIBRARY LOAN COPY

DO NOT TRANSFER TO ANOTHER PERSON

If you wish someone else to see this document, send in name with document and the library will arrange a loan.

OAK RIDGE NATIONAL LABORATORY
OPERATED BY
CARBIDE AND CARBON CHEMICALS COMPANY
A DIVISION OF UNION CARBIDE AND CARBON CORPORATION
UCC
POST OFFICE BOX P
OAK RIDGE, TENNESSEE

UNCLASSIFIED

C. R. Library

Copy No. 9

Oct. 1, 1953

ORNL-1283 Erratum

Title: General Principles of a Proton Recoil Fast-Neutron Spectrometer

Author: B. R. Gossick

✓ Page 8, In Fig. 1, angles PQR and PQO" should be shown as right angles.

✓ Page 16, Substitute attached revised Fig. 4.

✓ Page 17, Eq. 23 should read as follows:

$$\frac{\left\{\xi\lambda - \delta\lambda^2 + 1\right\}\left\{\left[\xi - (1+\delta)\lambda\right]^2 + \eta^2 + \eta^2\lambda^2\right\}}{\left\{(\xi - \delta\lambda)^2 + \eta^2 + 1\right\}^2\left\{\left[\xi - (1+\delta)\lambda\right]^2 + \eta^2\right\}}$$

✓ Page 21, Eq. 35 should read as follows:

$$\begin{aligned} t(r) &= t_1 && \text{for } 0 < |r| < \frac{t_2 - t_1}{2} \\ &= -r + \frac{t_1 + t_2}{2} && \text{for } \frac{t_2 - t_1}{2} < |r| < \frac{t_1 + t_2}{2} \\ &= 0 && \text{for } \frac{t_1 + t_2}{2} < |r| \end{aligned}$$

The same correction should be made on page 61 where Eq. 35 is repeated.

Page 24, Eq. 55 should read as follows:

$$b_2 = \left(4 + \frac{4}{g}\right)^{1/2} b_1$$

Page 27, Eq. 68 should read as follows:

$$L = \frac{1.65\pi}{g} S \overline{\Delta\rho_a^2}\ \overline{\Delta\rho_t^2}\ \bar{E}_n\ N(\bar{E}_n, \bar{\Omega}_1)\ \sigma(\bar{E}_n)\ \bar{R}$$

The factor R was similarly omitted in Eqs. 74, 80, 81, 82, 85, and 86 and in the calculations for Fig. 6. The revised figure is attached.

Page 37, Eq. 97: Minus sign should precede fraction on left side.

Page 43: To make page 43 agree with the revised Fig. 4, add an extra prime to each of the coordinates x, y, z, except for the expressions enclosed in brackets.

Page 51, Eq. A1.4 should read as follows:

$$\overline{\rho_a^2} = \overline{\rho_{ac}^2} + 2\,\overline{\rho_{ao}\,\rho_{ac}} + \overline{\rho_{ao}^2}$$

CENTRAL RESEARCH LIBRARY
DOCUMENT COLLECTION

[redacted]

ORNL-1283

This document consists of 62 pages.
Copy 9 of 309 copies. Series A

Contract No. W-7405-eng-26

Physics Division

GENERAL PRINCIPLES OF A PROTON RECOIL FAST-NEUTRON SPECTROMETER

B. R. Gossick

Date Issued

AUG 14 1952

OAK RIDGE NATIONAL LABORATORY
Operated by
CARBIDE AND CARBON CHEMICALS COMPANY
A Division of Union Carbide and Carbon Corporation
Post Office Box P
Oak Ridge, Tennessee

MARTIN MARIETTA ENERGY SYSTEMS LIBRARIES

3 4456 0360592 6

INTERNAL DISTRIBUTION

1. G. T. Felbeck (C&CCC)
2-3. Chemistry Library
4. Physics Library
5. Biology Library
6. Health Physics Library
7. Metallurgy Library
8-9. Training School Library
10. Reactor Experimental Engineering Library
11-14. Central Files
15. C. E. Center
16. C. E. Larson
17. W. B. Humes (K-25)
18. L. B. Emlet (Y-12)
19. A. M. Weinberg
20. E. H. Taylor
21. E. D. Shipley
22. A. H. Snell
23. F. C. VonderLage
24. R. C. Briant
25. J. A. Swartout
26. S. C. Lind
27. F. L. Steahly
28. A. Hollaender
29. M. T. Kelley
30. K. Z. Morgan
31. J. S. Felton
32. A. S. Householder
33. C. S. Harrill
34. C. E. Winters
35. D. S. Billington
36. D. W. Cardwell
37. E. M. King
38. E. O. Wollan
39. A. J. Miller
40. L. D. Roberts
41. R. N. Lyon
42. W. C. Koehler
43. W. K. Ergen
44. E. P. Blizard
45. M. E. Rose
46. D. D. Cowen
47. P. M. Reyling
48. J. L. Meem
49. R. G. Cochran
50. K. M. Henry
51. M. J. Skinner
52. G. H. Clewett
53-54. Central Files (O.P.)

EXTERNAL DISTRIBUTION

55-309. Given distribution as shown in TID-4500 under Instrumentation Category.

DISTRIBUTION PAGE TO BE REMOVED IF REPORT IS GIVEN PUBLIC DISTRIBUTION

Table of Contents

	Page
Summary	5
Introduction	6
Calculation of the Detection Rate	7
Calculation of the Range Error	19
Calculation of the Minimum Counting Time	30
Infinitely Thick Radiator	37
Acknowledgments	41
References	42
Appendices	43

List of Figures

Figure		Page
1	Geometry of Typical Experiment	8
2	Plot of g in Geiger's Equation ($R = kE^{g/2}$) for Paraffin Calculated from Range Data of Hirschfelder and Magee, Phys. Rev. 73 (1948)	11
3	Schematic Diagram of Absorbing Width t_o, Radiator Thickness t_1, and Detection Width t_2	13
4	Geometry of Typical Experiment Showing Transformation of Coordinates	16
5	Graph of Eq. (12), The Effective Radiator Thickness	18
6	Graph of Minimum Counting Time vs Energy Width at Half Maximum	34
7	Graph of Minimum Counting Time vs Energy Width at Half Maximum	35
8	Graph of Minimum Counting Time vs Energy Width at Half Maximum	36

GENERAL PRINCIPLES OF A PROTON RECOIL FAST-NEUTRON SPECTROMETER

B. R. Gossick

Summary

A general equation for calculating the neutron energy spectrum from proton recoil counting data is derived. This equation is optimized subject to a constant total error to determine the most favorable experimental conditions. Feasible accuracy is illustrated by presenting a family of curves of the counting time (required for one point on a spectrum) plotted against total error with source intensity as a parameter. The calculations apply only to a "good geometry" experiment with a point source. The subject is treated for the most part in terms of a thin radiator, but the calculations apply equally well for the case of a thick radiator by a simple extension which is outlined.

Introduction

A proton recoil instrument has the dual purpose of obtaining information about both neutron energy and neutron intensity. Since the measured intensity can be increased by only three means (1) widening the collimator, (2) making the radiator thicker, and (3) increasing the counter detection width, the information about intensity can be gained only by sacrificing information about energy. This is shown by the facts that enlarging the collimator increases the uncertainty in the collision angle, making the radiator thicker increases the uncertainty in the beginning of the range, and expanding the counter detection width increases the uncertainty in the end of the range.

That such a relationship exists between energy and intensity errors is not surprising as it is apparently inherent in the general principles of measurements. What is of interest is the magnitude of this relationship for particular types of measurements since the quantitative expression for this magnitude provides a criterion of feasibility for the experimenter. The following paragraphs are mainly devoted to determining the relationship between energy and intensity errors for the special case of a proton recoil instrument with a collimator. However, in order to establish the connection between these errors it is first necessary to determine the counting rate and the separate error contributions.

Instruments which fall into the category considered here have been reported recently by B. E. Watt[1], Los Alamos Scientific Laboratory; D. L. Hill[2], Argonne National Laboratory; B. B. Kinsey, S. G. Cohen, and J. Dainty[3], Great Britain; B. L. Cohen and C. E. Falk[4], Carnegie Institute of Technology; R. G. Cochran, B. R. Gossick, K. Henry, and F. J. Muckenthaler, Oak Ridge National Laboratory, the prototype of which was described by Gossick and Henry[5].

Calculation of the Detection Rate

The essential geometric details of a proton recoil instrument are portrayed in Fig. 1. As shown, the neutrons are considered to be emerging from a point, and the radiator and collimator are circular with equal radii. "Good geometry" is assumed, i.e., separation distances b_1 and b_2 are large compared to a. If the radiator area were small compared to the collimator area, recoil protons could be treated as coming from a point source, simplifying the problem. Simplication could also be attained by making b_1 large compared to b_2 so that the neutron emission angle λ may be neglected. However, both of these simplifications involve a loss of intensity which cannot be afforded. n-p scattering is treated as being elastic and isotropic in the center of mass system. According to Segrè[6] this assumption is good up to 14 Mev, below which there is no departure from spherical symmetry in the scattering. The departure from spherical symmetry[6] increases with energy, and at 27 Mev $\frac{\sigma(\pi)}{\sigma(\frac{\pi}{2})} = 1.28 \pm .008$.

Let $N(E_n, \Omega_1)$ denote the emission rate of neutrons per unit energy per unit solid angle, where E_n denotes the neutron energy and Ω_1 the solid angle. The n-p process rate in a small element within the radiator is given by

$$df = N(E_n, \Omega_1)\ S\ \sigma(E_n)\ t(R, \lambda, \gamma_p)\ dE_n d\Omega_1 \quad , \qquad (1)$$

where $\sigma(E_n)$ represents the hydrogen scattering cross section, S is the density of hydrogen atoms in the radiator, and $t(R, \lambda, \gamma_p)$ the effective radiator thickness as a function of proton range R, neutron emission angle λ, and proton range

UNCLASSIFIED
DWG. 15153

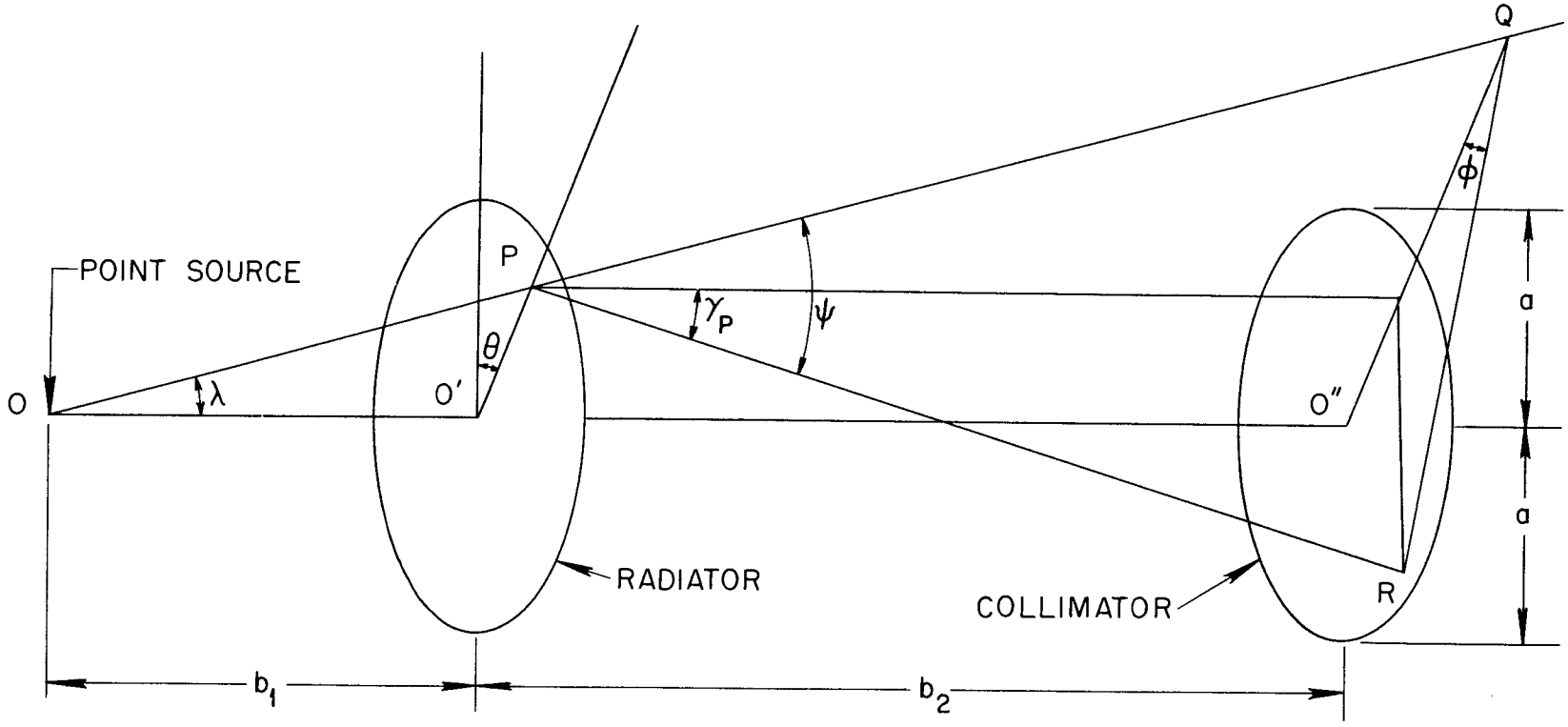

Angels PQR and PQO should be shown as right angels.
(correction made per notice dated 11/1/59)

Fig. 1 Geometry of Typical Experiment.

obliquity angle γ_p. Since

$$d\Omega_1 = \sin\lambda \; d\lambda \; d\theta \tag{2}$$

(1) may be rewritten as

$$df = S\, N(E_n, \Omega_1)\, \sigma(E_n)\, t(R, \lambda, \gamma_p) \sin\lambda \; d\lambda \; d\theta \; dE_n \; . \tag{3}$$

Assuming isotropic scattering in the center of mass system, the fraction of df which is scattered into a small solid angle $d\Omega_2$ equals

$$\frac{\sin 2\psi \; d2\psi \; d\varphi}{4\pi} = \frac{\sin\psi \; \cos\psi \; d\psi \; d\varphi}{\pi} \tag{4}$$

When $d\Omega_2$ is directed toward the collimator, the contribution of the interval $(E_n, E_n + dE_n; \theta, \theta + d\theta; \lambda, \lambda + d\lambda; \psi, \psi + d\psi; \varphi, \varphi + d\varphi)$ to the detection rate may be expressed as

$$dL = \frac{S}{\pi} N(E_n, \Omega_1)\, \sigma(E_n)\, t(R, \lambda, \gamma_p) \sin\lambda \; \sin\psi \; \cos\psi \; d\theta \; d\lambda \; d\psi \; d\varphi \; dE_n \; . \tag{5}$$

The counting rate is obtained by integrating (5) over the contributing intervals of the arguments, and as (5) is the partial weight for a recoil being detected, it provides the distribution function for determining the errors in the proton range. Since neither $t(R, \lambda, \gamma_p)$ nor the errors are functions of θ because of symmetry, it is convenient to integrate (5) with respect to θ at the outset and ignore it in subsequent calculations. Thus

$$dL = 2S\, N(E_n, \Omega_1)\, \sigma(E_n)\, t(R, \lambda, \gamma_p) \sin\lambda \; \sin\psi \; \cos\psi \; d\lambda \; d\psi \; d\varphi \; dE_n \; . \tag{6}$$

By Geiger's Law the range of a recoil proton with collision angle, ψ, may be expressed in terms of neutron energy E_n as

$$R = k\, E_n^{g/2} \cos^g \psi \ , \tag{7}$$

where k is a constant and g is a very slowly varying function of proton energy. Since we always consider here the interval of resolution for the measurement of one energy point, which is small, we may consider g as being constant in that interval. Figure 2 is a plot of g for paraffin, which was calculated from the range-energy tables of Hirschfelder and Magee [7].

It follows from (7) that

$$dR = \frac{g}{2} \frac{R}{E_n} dE_n \ , \tag{8}$$

so that

$$dE_n = \frac{2E_n}{gR} dR \ , \tag{9}$$

which, when substituted into (6), yields

$$dL = \frac{4S}{g} \frac{E_n}{R} N(E_n, \Omega_1)\sigma(E_n)t(R, \lambda, \gamma_p) \sin\lambda \sin\psi \cos\psi \, d\lambda \, d\psi \, d\varphi \, dR \tag{10}$$

Since "good geometry" is assumed, angle λ is always small. Hence sin λ may be replaced by λ. Then by using "good geometry" (10) may be approximated by

$$dL = \frac{4S}{g} \frac{E_n}{R} N(E_n, \Omega_1)\sigma(E_n)t(R, \lambda, \gamma_p) \lambda \sin\psi \cos\psi \, d\lambda \, d\psi \, d\varphi \, dR \ . \tag{11}$$

The effective radiator thickness has been treated by Cohen and Falk[4] as a function of neutron energy by considering only head-on collisions so that

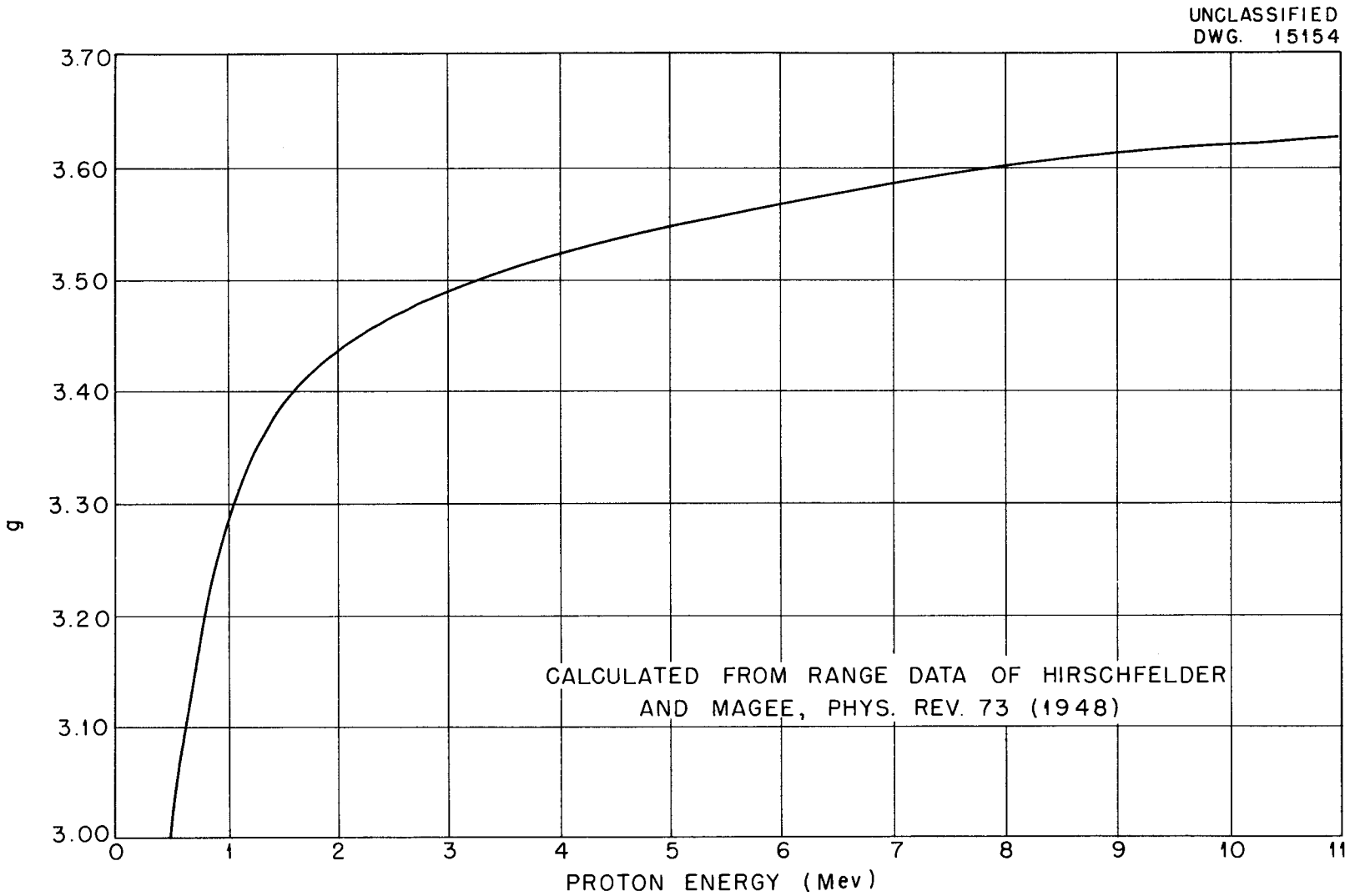

Fig. 2. Plot of g in Geiger's Equation $g = 2\,\frac{d(\ln R)}{d(\ln E)}$ for Paraffin.

neutron and proton energy are interchangeable. The function for the effective radiator thickness used here is essentially the same because the dependence on λ and γ_p can be neglected with "good geometry". To show this, it is convenient to commence with Fig. 3. t_o, t_1, and t_2 refer to distances in terms of the stopping power of the hydrogenous radiator. Only the radiator, shown as t_1 in Fig. 3, is hydrogenous, and the values of t_o and t_2 must be converted from range energy data. Protons are produced in t_1, and some traverse the intervening distance and come to rest in the detection width t_2. t_o represents the total stopping power of material between t_1 and t_2 in equivalent centimeters of the radiator material. That the end of the range is within t_2 may be made certain by either a coincidence - - anti-coincidence circuit, or by using a differential counter in conjunction with a pulse height discriminator. The detection width t_2 must be calculated from the characteristics of the particular detection apparatus employed. In obtaining $t(R, \lambda, \gamma_p)$ we let t_1 and t_2 represent radiator thickness and detection width interchangeably, but choose them so that $t_1 \leq t_2$. Taking into account only head-on collisions and considering all possible ranges beginning in the radiator and terminating in the detection zone, the following function can be readily obtained.

$$\left.\begin{array}{lll} t(R) = 0 & \text{for} & R < t_o \\ \quad = R - t_o & \text{for} & t_o < R < t_o + t_1 \\ \quad = t_1 & \text{for} & t_o + t_1 < R < t_o + t_2 \\ \quad = -R + t_o + t_1 + t_2 & \text{for} & t_o + t_2 < R < t_o + t_1 + t_2 \\ \quad = 0 & \text{for} & R > t_o + t_1 + t_2 \end{array}\right\} \qquad (12)$$

UNCLASSIFIED
DWG. 15155

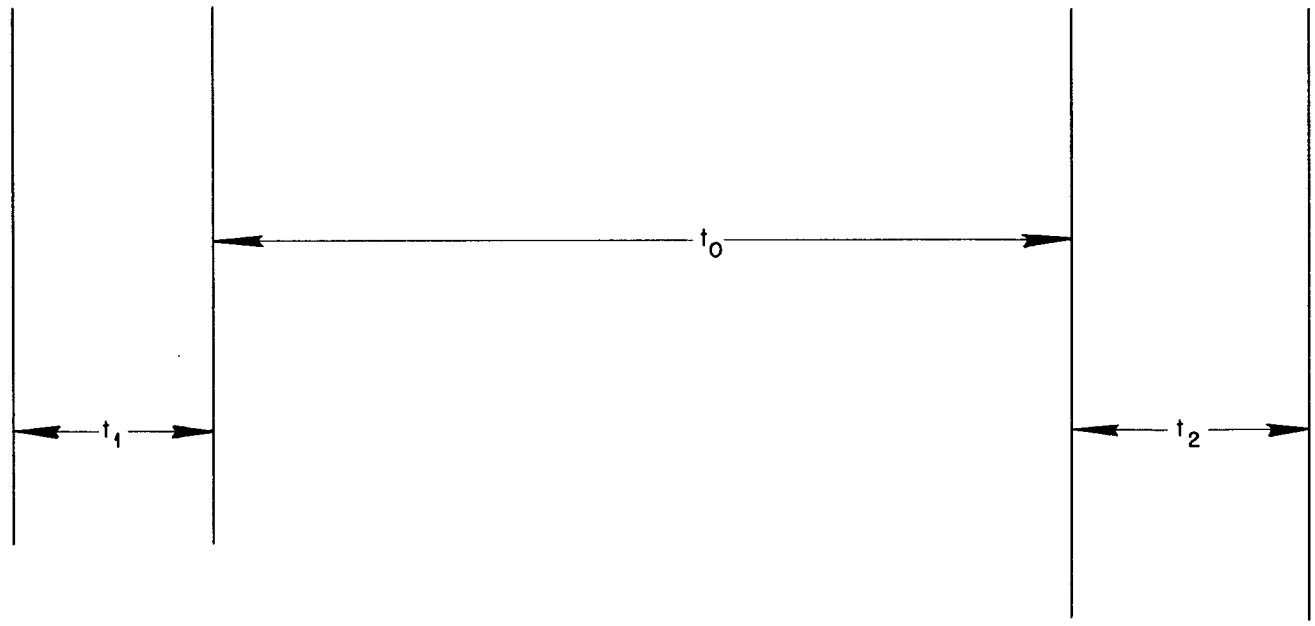

Fig. 3 Schematic Diagram of Absorbing Width t_0, Radiator Thickness t_1 And Detector Width t_2.

Having obtained t(R) it is evident that R must be replaced by the projected range R cos γ_p in the general case, and the thickness enlarged by the factor $\frac{1}{\cos \lambda}$ for neutrons with oblique incidence. Then in general

$$\left.\begin{aligned}
t(R, \lambda, \gamma_p) &= 0 && \text{for } R \cos \gamma_p < t_o \\
&= \frac{R \cos \gamma_p - t_o}{\cos \lambda} && \text{for } t_o < R \cos \gamma_p < t_o + t_1 \\
&= \frac{t_1}{\cos \lambda} && \text{for } t_o + t_1 < R \cos \gamma_p < t_o + t_2 \\
&= \frac{-R \cos \gamma_p + t_o + t_1 + t_2}{\cos \lambda} && \text{for } t_o + t_2 < R \cos \gamma_p < t_o + t_1 + t_2 \\
&= 0 && \text{for } R \cos \gamma_p > t_o + t_1 + t_2
\end{aligned}\right\} \quad (13)$$

Since λ and γ_p are small with "good geometry", we are at liberty to replace $t(R, \lambda, \gamma_p)$ in (11) by its value in (12).

As an approximation $\frac{E_n}{R} N(E_n, \Omega_1)\sigma(E_n)$ is now replaced in (11) by its average in the interval of resolution. $\overline{\Omega}_1$ is determined from the geometry of the experiment while $\overline{E}_n$ is determined by the equation

$$\overline{R} = R(\overline{E}_n) = t_o + \frac{t_1 + t_2}{2} \quad . \tag{14}$$

Employing the substitutions in (11) indicated above give for the partial contribution to the detection rate

$$dL = \frac{4S}{g} \frac{\overline{E}_n}{\overline{R}} N(\overline{E}_n, \overline{\Omega}_1)\sigma(\overline{E}_n)t(R) \lambda \sin \psi \cos \psi \, d\lambda \, d\psi \, d\varphi \, dR \tag{15}$$

$$= K(\overline{E}_n)t(R) \lambda \sin \psi \cos \psi \, d\lambda \, d\psi \, d\varphi \, dR \quad . \tag{16}$$

It is now advantageous to make a transformation of coordinates, eliminating ψ and φ in favor of ξ and η, where

$$\xi = \frac{x}{b_2} \tag{17}$$

and

$$\eta = \frac{y}{b_2} \quad . \tag{18}$$

Coordinates x and y are shown in Fig. 4. Since the maximum values of both x and y equal a, then ξ and η are both small with "good geometry". In order to make the notation more concise, let

$$\alpha = \frac{a}{b_2}$$

and

$$\gamma = \frac{b_1}{b_2} \quad . \tag{20}$$

We use the Jacobian determinant $|J|$ to affect the transformation of coordinates.

$$d\varphi \, d\psi = |J| \, d\xi \, d\eta \quad , \tag{21}$$

where

$$|J| = \begin{vmatrix} \frac{\partial \psi}{\partial \xi} & \frac{\partial \psi}{\partial \eta} \\ \frac{\partial \varphi}{\partial \xi} & \frac{\partial \varphi}{\partial \eta} \end{vmatrix} \quad . \tag{22}$$

A calculation of $|J|$ is made in Appendix 1, the result of which is

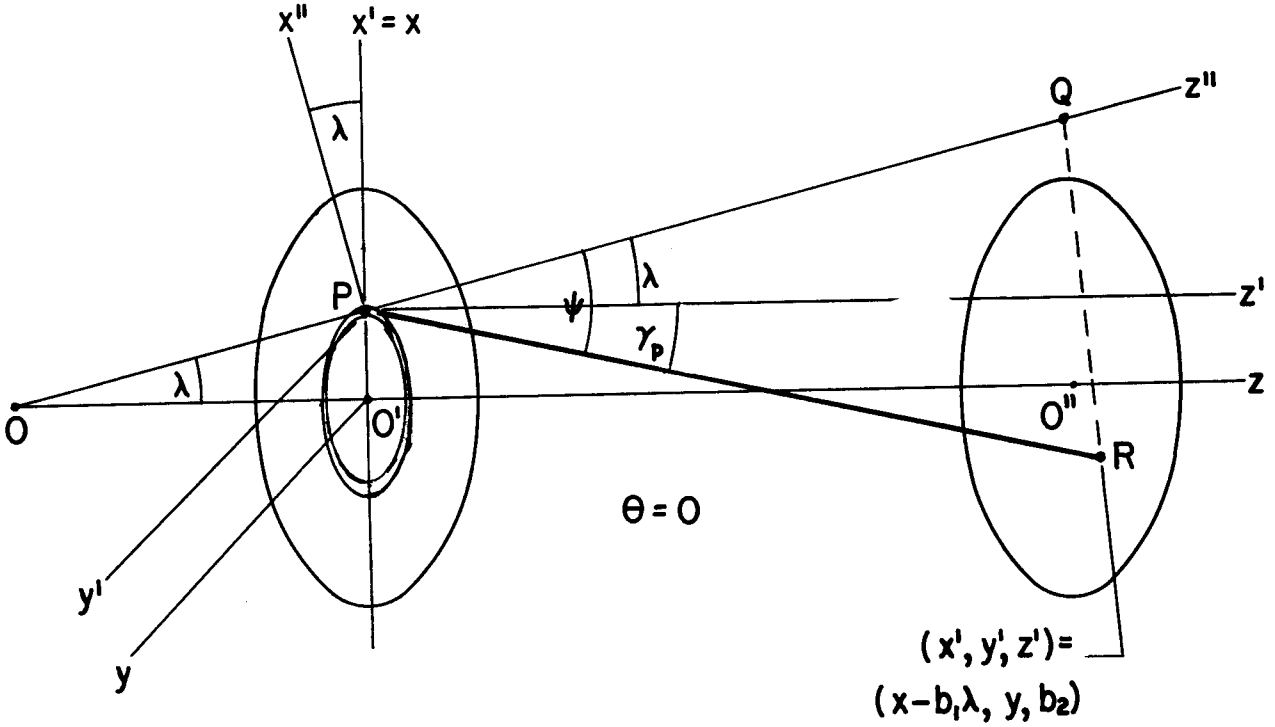

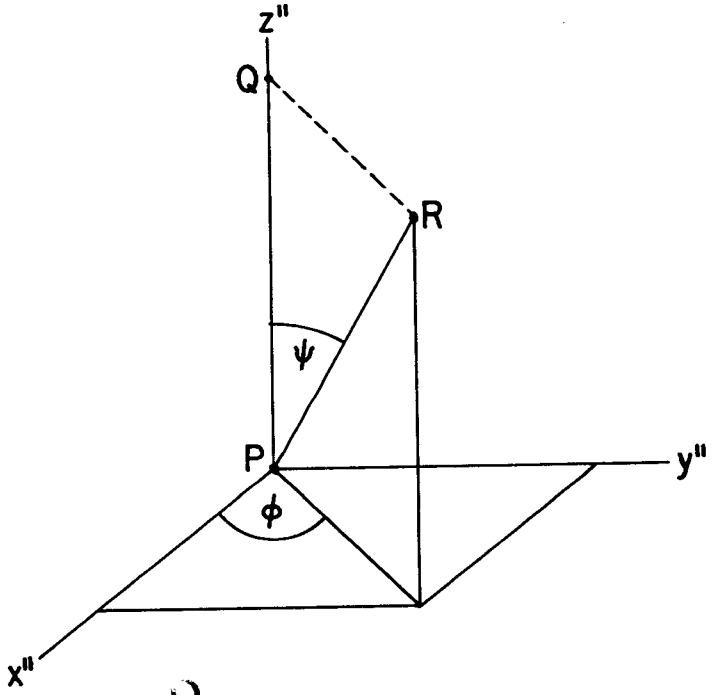

Fig. 4. (Revised) Geometry of typical experiment showing transformation of coordinates.

$\sin\psi\cos\psi\ |J| =$

$$\frac{\left\{\xi\lambda - \delta\lambda^2 + 1\right\}\left\{\left[\xi - (1+\delta)\lambda\right]^2 + \eta^2 + \eta^2\lambda^2\right\}}{\left\{(\xi - \delta\lambda)^2 + \eta^2 + 1\right\}^2\left\{\left[\xi - (1+\delta)\lambda\right]^2 + \eta^2\right\}} \tag{23}$$

With "good geometry" it is possible to neglect terms of order ξ^2, and when this is done, it may be seen that (23) equals unity. Therefore (16) may be rewritten as

$$dL = K(\overline{E}_n)t(R)\,\lambda\, d\lambda\, d\xi\, d\eta\, dR \quad . \tag{24}$$

Thus

$$L = K(\overline{E}_n)\int_{R=t_o}^{R=t_o+t_1+t_2}\int_{\lambda=0}^{\lambda=a/b_1}\int_{\eta=-\alpha}^{\eta=\alpha}\int_{\xi=-\sqrt{\alpha^2-\eta^2}}^{\xi=\sqrt{\alpha^2-\eta^2}} t(R)\,\lambda\, d\xi\, d\eta\, d\lambda\, dR \tag{25}$$

The integral of (25) over the dimensional coordinates λ, η, and ξ is carried out in Appendix 2. The following result is obtained

$$L = K(\overline{E}_n)\ \frac{\pi}{2}\left(\frac{a}{b_1}\right)^2\left(\frac{a}{b_2}\right)^2\int_{R=t_o}^{R=t_o+t_1+t_2} t(R)dR \tag{26}$$

The final integral is given by the area of the trapezoid in Fig. 5. Thus

$$\int_{R=t_o}^{R=t_o+t_1+t_2} t(R)dR = t_1\ t_2 \tag{27}$$

UNCLASSIFIED
DWG. 15157

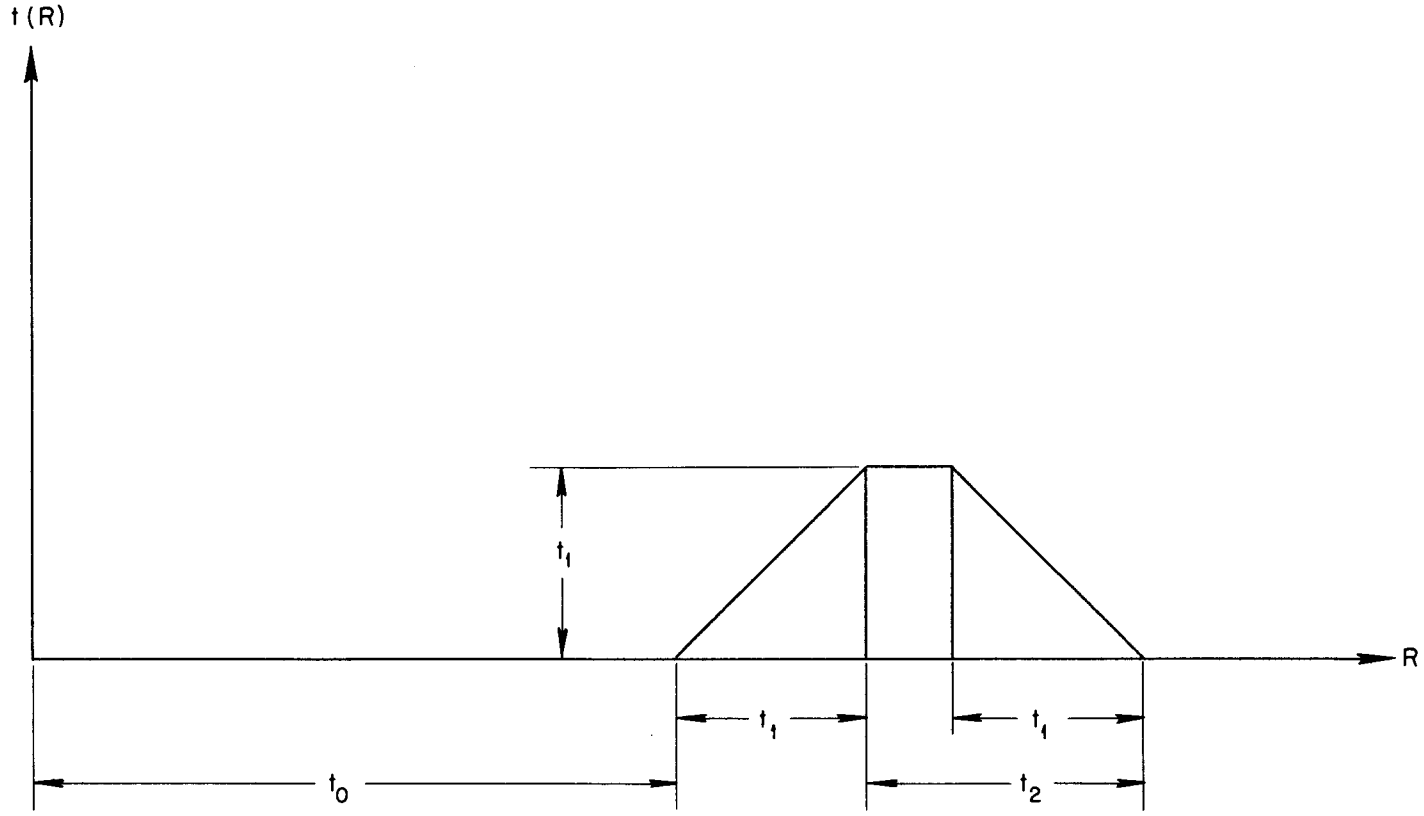

Fig. 5 Graph of Equation (12), The Effective Radiator Thickness.

Therefore

$$\left.\begin{aligned} L &= K(\bar{E}_n)\ \frac{\pi}{2}\left(\frac{a}{b_1}\right)^2\left(\frac{a}{b_2}\right)^2\ t_1\ t_2 \\ &= \frac{2\pi S}{g}\left(\frac{a}{b_1}\right)^2\left(\frac{a}{b_2}\right)^2 t_1\ t_2\ \frac{\bar{E}_n}{\bar{R}}\ N(\bar{E}_n, \bar{\Omega}_1)\ \sigma(\bar{E}_n) \end{aligned}\right\} \qquad (28)$$

Equation (28) gives the counting rate, and from the experimentally obtained value of L, one can immediately solve for $N(\bar{E}_n, \bar{\Omega}_1)$.

Calculation of the Range Error

The following error components in the proton range must be considered: (1) energy straggling, (2) angular straggling, (3) radiator and detection width errors. The first error is independent of the instrument, and the value for this error given by Livingston and Bethe[8] always applies. The second error is due to uncertainties in the neutron emission angle λ, the n-p scattering angle ψ, and the range obliquity angle γ_p; it is an instrumental error, depending upon the dimensions a, b_1, and b_2. The third error is due to the uncertainty in the beginning of the range within the radiator and the uncertainty in the end of the range in the detection width. This again is an instrumental error, and it depends upon the dimensions t_o, t_1, and t_2. The partial contribution to the detection rate given by (24) provides the distribution function for calculating the second and third errors in the range.

The third error enters into the partial weight through the factor t(R) which is independent of dimension coordinates ξ, η, and λ using "good

geometry". Let ρ_t denote the fractional range error due to the radiator and detection width, and ρ_a the fractional range error due to angular straggling. Let ρ_t now represent the range error due to t_1 and t_2 which would occur if the path of the proton were along $\overline{PQ}$ in Fig. 4. However, on the basis of "good geometry", $\overline{PQ}$ and $\overline{O'O''}$ are considered here as being interchangeable so that ρ_t may be considered as a function $\rho_t(R)$. The error ρ_a then is made to account for the proton path being along $\overline{PR}$ rather than $\overline{PQ}$. In the latter case $\overline{PQ}$ is not replaced by $\overline{O'O''}$, and ρ_a is considered as a function $\rho_a(\xi, \eta, \lambda)$. Although (24) supplies the partial weight in both cases, the two errors are independent of each other because they depend upon different variables. Hence, we may write

$$P_a(\xi, \eta, \lambda) = A_a \lambda \tag{29}$$

as the distribution function for "angular straggling", where

$$A_a = \frac{2}{\pi} \left(\frac{b_1}{a}\right)^2 \left(\frac{b_2}{a}\right)^2 \tag{30}$$

is the normalizing constant.

Similarly, the distribution function for the radiator and detection width error ρ_t may be expressed as

$$P_t(R) = A_t \, t(R) \tag{31}$$

where

$$A_t = \frac{1}{t_1 \, t_2} \tag{32}$$

is the normalizing constant.

To simplify calculations involving (31), let

$$R = t_o + \frac{t_1 + t_2}{2} + r \tag{33}$$

$$dR = dr \tag{34}$$

$$\left.\begin{aligned} t(r) &= t_1 \\ &= t_1 && \text{for} \quad 0 < |r| < \frac{t_2 - t_1}{2} \\ &= -r + \frac{t_1 + t_2}{2} && \text{for} \quad \frac{t_2 - t_1}{2} < |r| < \frac{t_1 + t_2}{2} \\ &= 0 && \text{for} \quad \frac{t_1 + t_2}{2} < |r| \end{aligned}\right\} \tag{35}$$

Changes per Notice 11/1/53

Then

$$P_t(r) = A_t \, t(r) \, . \tag{36}$$

By making this transformation, the convenient relation

$$\overline{\rho_t} = A_t \int_{-\infty}^{\infty} \rho_t(r) \, t(r) \, dr = 0 \tag{37}$$

is obtained. The combined range error due to ρ_a and ρ_t is then $\rho = \rho_a + \rho_t$, and the combined mean square deviation may be obtained as follows.

$$\overline{\Delta\rho^2} = \overline{(\rho - \overline{\rho})^2} = \int_0^{a/b_1} \int_{-\alpha}^{\alpha} \int_{-\sqrt{\alpha^2 - \eta^2}}^{\sqrt{\alpha^2 - \eta^2}} \int_{-\infty}^{\infty} (\rho_a - \overline{\rho_a} + \rho_t)^2 \, P_t(r) \, P_a(\xi, \lambda, \eta) \, dr \, d\xi \, d\eta \, d\lambda \tag{38}$$

$$= \overline{\rho_a^2} - (\overline{\rho_a})^2 + \overline{\rho_t^2} \tag{39}$$

$$= \overline{\Delta\rho_a^2} + \overline{\Delta\rho_t^2} \tag{40}$$

where $\overline{\rho_t^2}$ is the same as $\overline{\Delta\rho_t^2}$ because of the transformation made by (33). For convenience, we shall proceed to calculate $\overline{\rho_a}$, $\overline{\rho_a^2}$ and $\overline{\rho_t^2}$ separately.

The proton range is given by (7), which may be written as

$$R = k\, E_n^{g/2} (1 - \sin^2 \psi)^{g/2} \tag{41}$$

and with good geometry, since ψ is always small, R may be approximated by

$$R = k\, E_n^{g/2} (1 - g/2 \sin^2 \psi). \tag{42}$$

Since $k\, E_n^{g/2}$ represents the range $R(E_n)$, we shall replace it by

$\bar{R} = t_o + \frac{t_1 + t_2}{2}$ as we did in (14).

$$R = \bar{R} (1 - g/2 \sin^2 \psi) . \tag{43}$$

The apparent or projected range is $R \cos \gamma_p$ which is denoted here by R_p.

$$R_p = \bar{R} (1 - g/2 \sin^2 \psi) \cos \gamma_p \tag{44}$$

$$\cong \bar{R} (1 - g/2 \sin^2 \psi - 1/2 \sin^2 \gamma_p) \tag{45}$$

Then, by (45) the fractional error in the range due to "angular straggling" may be written as

$$\rho_a = \frac{R_p - \bar{R}}{\bar{R}} = - g/2 \sin^2 \psi - 1/2 \sin^2 \gamma_p \tag{46}$$

Since the first term represents the fractional decrement due to the scattering angle ψ, and the second term represents the decrement due to the angle of obliquity γ_p, we shall keep the two terms separate, distinguishing them by the

Added per Notice 11/1/53

Page 23, At top of page attach the following note:

In the range error calculation due to collision angle starting with Eq. 47, the coordinates ξ and η should be interchanged to agree with Fig. 4. Because of symmetry, interchanging these coordinates does not affect the outcome of the calculations.

$$\sin^2 \psi = \xi^2 + \left[(1 + \delta)\ \lambda - \eta\right]^2 , \tag{47}$$

and

$$\sin^2 \gamma_p = \xi^2 + (\delta \lambda - \eta)^2 . \tag{48}$$

Therefore

$$\rho_{ac} = - g/2 \left\{ \xi^2 + \left[(1 + \delta)\ \lambda - \eta\right]^2 \right\} \tag{49}$$

and

$$\rho_{ao} = - 1/2 \left[\xi^2 + (\delta \lambda - \eta)^2 \right] \tag{50}$$

Since $\overline{\rho_a} = \overline{\rho_{ac}} + \overline{\rho_{ao}}$, the two contributions are determined separately. This makes the calculation somewhat more concise, and it is interesting to be able to compare the two terms. This calculation is carried out in Appendix 3, and the results are stated below.

$$\overline{\rho_{ac}} = - \frac{g}{4}\ a^2 \left[\left(\frac{1}{b_1} + \frac{1}{b_2}\right)^2 + \left(\frac{1}{b_2}\right)^2 \right] , \tag{51}$$

$$\overline{\rho_{ao}} = - \frac{1}{2} \left(\frac{a}{b_2}\right)^2 \tag{52}$$

$$\overline{\rho_a} = - \frac{a^2}{4} \left[\frac{g}{b_1^2} + \frac{2g}{b_1 b_2} + \frac{2g + 2}{b_2^2} \right] . \tag{53}$$

It is interesting to note that $\overline{\rho_{ao}}$ is independent of the separation distance b_1. In a later calculation it is shown that it is profitable to make b_1 about half the value of b_2, in which case $\overline{\rho_{ac}} = 5g\ \overline{\rho_{ao}}$, and since $g \sim 3$, $\overline{\rho_{ac}} \sim 15\ \overline{\rho_{ao}}$.

Unfortunately, the separate contributions of ρ_{ac} and ρ_{ao} cannot be identified in the expression for $\overline{\Delta\rho_a^2}$ since the latter contains cross products of ρ_{ac} and ρ_{ao}.

The calculation of $\overline{\Delta\rho_a^2}$ is carried out in Appendix 4. The result is stated below.

$$\overline{\Delta\rho_a^2} = \left(\frac{g^2}{48} + \frac{g}{24} + \frac{1}{6}\right)\left(\frac{a}{b_2}\right)^4 + \left(\frac{g^2}{8} + \frac{g}{24}\right)\left(\frac{a}{b_2}\right)^2\left(\frac{a}{b_1} + \frac{a}{b_2}\right)^2$$

$$+ \frac{g^2}{48}\left(\frac{a}{b_1} + \frac{a}{b_2}\right)^4 + \frac{g}{4}\left(\frac{a}{b_2}\right)^3\left(\frac{a}{b_1} + \frac{a}{b_2}\right) \quad . \tag{54}$$

The optimum relation between b_1 and b_2 is that which provides a maximum counting rate for a constant error $\overline{\Delta\rho_a^2}$. It is convenient to calculate first the corresponding relations for constant errors $\overline{\rho_a}$ and $\rho_{a\,max}$. Using the familiar method of Lagrangian multipliers one obtains

$$\cancel{b_2 = \sqrt{4 + \frac{1}{g}}\; b_1} \quad , \qquad b_2 = \left(4 + \frac{4}{g}\right)^{1/2} b_1 \tag{55}$$

for constant $\rho_{a\,max}$ *change per notice 11/1/53*

and $$b_2 = \sqrt{2 + \frac{2}{g}}\; b_1 \quad , \tag{56}$$

for constant $\overline{\rho_a}$.

On the basis of (55) and (56), $\frac{1}{b_1}$ is now replaced in (54) by $\frac{2}{b_2} + \frac{\Delta}{b_2}$ where Δ is considered to be small. The optimum relation between b_1 and b_2 for $\overline{\Delta\rho_a^2}$ = constant is calculated in Appendix 5. All terms in Δ^2 and of higher order are neglected. The following relation is obtained.

$$\frac{b_2}{b_1} = \frac{-2q_1 + 6q_2 + 270q_3 - 2q_4}{6q_2 + 108q_3 + q_4} \tag{57}$$

where

$$q_1 = \frac{g^2}{48} + \frac{g}{24} + \frac{1}{6} \tag{58}$$

$$q_2 = \frac{g^2}{8} + \frac{g}{24} \tag{59}$$

$$q_3 = \frac{g^2}{48} \tag{60}$$

$$q_4 = \frac{g}{4} \tag{61}$$

Since g varies slowly with proton energy, the ratio $\frac{b_2}{b_1}$ is somewhat energy dependent in (57). If this is neglected and g is replaced by 3 as an approximation, then $\frac{1}{b_1} = \frac{1.96}{b_2}$, which justifies our having replaced $\frac{1}{b_1}$ by $\frac{2}{b_2}(1 + \frac{\Delta}{2})$ in (54). As $\Delta \sim -0.04$, the higher order terms are small compared to Δ.

Setting g equal to 3, the value of $\Delta\overline{\rho_a^2}$ for the optimum relation between b_1 and b_2 (taken as $b_2 = 2b_1$) is

$$\Delta\overline{\rho_a^2} = 29.1 \left(\frac{a}{b_2}\right)^4 . \tag{62}$$

Substituting (62) into (28) yields the counting rate, optimized with respect to b_1 and b_2.

$$L = \frac{\pi}{3.64} \frac{S}{g} \Delta\overline{\rho_a^2}\, t_1 t_2 \frac{\bar{E}_n}{\bar{R}} N(\bar{E}_n, \bar{\Omega}_1)\, \sigma(\bar{E}_n) . \tag{63}$$

The next range error to be considered is that due to the radiator and detection widths, which was introduced as ρ_t in (37). On the basis of (14) and

(33) it follows that

$$\rho_t(r) = \frac{r}{\bar{R}} = \frac{r}{t_o + \frac{t_1 + t_2}{2}} \quad . \tag{64}$$

Thus

$$\overline{\Delta\rho_t^2} = 2A_t \int_0^{\frac{t_1 + t_2}{2}} \rho_t^2 \; t(r)\, dr \quad . \tag{65}$$

The value of the above integral is calculated in Appendix 6. The result is given below.

$$\overline{\Delta\rho_t^2} = \frac{t_1^2 + t_2^2}{12(\bar{R})^2} = \frac{t_1^2 + t_2^2}{12(t_o + \frac{t_1 + t_2}{2})^2} \quad . \tag{66}$$

The optimum relation between t_1 and t_2 is $t_1 = t_2$, as may be easily verified by maximizing the counting rate (63) subject to constant $\overline{\Delta\rho_t^2}$.

Since background depends upon particular experimental conditions external to the equipment, it cannot be treated in general. By neglecting background we have implicitly assumed that our instrument discriminates perfectly against background. Thus the optimum relation $t_1 = t_2$ holds only for an ideal instrument. It should be recognized that background intensity may necessitate making the detection width less than the radiator width, a practical limitation making it impossible to utilize the benefit of the relation $t_1 = t_2$. Then, for an ideal instrument only

$$\overline{\Delta\rho_t^2} = \frac{t_1^2}{6(\bar{R})^2} = \frac{1}{6}\left(\frac{t_1}{t_o + t_1}\right)^2 \quad , \tag{67}$$

which provides a counting rate

$$L = \frac{1.65\,\pi}{g}\; S\; \overline{\Delta\rho_a^2}\; \overline{\Delta\rho_t^2}\; \bar{E}_n\, N(\bar{E}_n, \bar{\Omega}_1)\, \sigma(\bar{E}_n)\; .\; \bar{R} \tag{68}$$

Changed per notice 11/1/53

The error in the range due to the instrument is now obtained by inserting (54) and (66) into (40)

$$\left.\begin{aligned} \overline{\Delta\rho^2} = {} & q_1 \left(\frac{a}{b_2}\right)^4 + q_2 \left(\frac{a}{b_2}\right)^2 \left(\frac{a}{b_1} + \frac{a}{b_2}\right)^2 + q_3 \left(\frac{a}{b_1} + \frac{a}{b_2}\right)^4 \\ & + q_4 \left(\frac{a}{b_2}\right)^3 \left(\frac{a}{b_1} + \frac{a}{b_2}\right) + \frac{t_1^2 + t_2^2}{12\left(t_o + \frac{t_1 + t_2}{2}\right)^2} \end{aligned}\right\} \tag{69}$$

The total error in the range must contain a term which accounts for energy straggling. This error is caused by the mechanism by which the proton energy is attenuated in traversing a substance. The proton suffers many small decrements of energy to electrons in the stopping substance. There are statistical fluctuations in the number of interactions and the amount of energy transfer per interaction. Thus, there are statistical fluctuations in the ranges of protons emitted from a monochromatic source, and this is consequently an error which is independent of the instrument. The total mean square deviation in the range may be expressed as the sum of (69) and the mean square deviation in the range due to energy straggling $\overline{\Delta\rho_s^2}$. By employing equations (791a), (792b), (793) and (793a) of ref. 8, one can obtain

$$\overline{\Delta\rho_s^2} = \frac{2}{\pi}\left(\frac{R_{ex} - R_o}{R_o}\right)^2 = \frac{\overline{(R - R_o)^2}}{R_o^2} \; . \tag{70}$$

The ratio $\frac{R_{ex} - R_o}{R_o}$ has been recently tabulated by Bethe[9], and earlier in ref. 8. The total range error is thus given by the sum of (69) and (70). Let this sum be denoted by

$$\overline{\Delta \rho^2_{tot}} = \overline{\Delta \rho^2_s} + \overline{\Delta \rho^2_a} + \overline{\Delta \rho^2_t} \quad . \tag{71}$$

By Geiger's Law the corresponding energy error is

$$\overline{\epsilon^2} = \left(\frac{2}{g}\right)^2 \overline{\Delta \rho^2_{tot}} \quad . \tag{72}$$

The optimum relation between b_1 and b_2 and the corresponding relation between t_1 and t_2 have been determined, but not the optimum relation between b_1 and t_1. That may be obtained by optimizing the counting rate (68) subject to (71) being constant. Of course (71) in this case represents the error when $b_1 = \frac{b_2}{2}$ and $t_1 = t_2$. Since $\overline{\Delta \rho^2_s}$ has nothing to do with the counting rate, it drops out of the calculation. The result is that $\overline{\Delta \rho^2_a}$ should equal $\overline{\Delta \rho^2_t}$, giving the relation

$$13.3 \left(\frac{a}{b_2}\right)^2 = \frac{t_1}{t_o + t_1} \quad . \tag{73}$$

Therefore the maximum counting rate may be written as

$$L_{max} = \frac{1.65\ \pi\ S}{g} \left(\overline{\Delta \rho^2_t}\right)^2 \bar{E}_n\ N(\bar{E}_n, \bar{\Omega}_1)\ \sigma(\bar{E}_n)\ \bar{R} \tag{74}$$

where

$$\overline{\Delta\rho_t^2} = \frac{1}{6} \left(\frac{t_1}{t_o + t_1}\right)^2 \quad , \tag{67}$$

$$13.3 \left(\frac{a}{b_2}\right)^2 = \frac{t_1}{t_o + t_1} \quad , \tag{73}$$

$$b_1 = \frac{b_2}{2}$$

$$t_1 = t_2 \quad .$$

Thus, for a given source intensity $N(\bar{E}_n, \bar{\Omega}_1)$, the maximum counting rate L_{max} cannot be increased except by increasing either the range error or the hydrogen density in the radiator S. Typical values of S are:

$$S = 7.65 \times 10^{22} \quad \text{(paraffin)}$$

$$S = 6.4 \times 10^{22} \quad \text{(glycerol tristearate)}$$

$$S = 4.92 \times 10^{22} \quad \text{(polystyrene)} \quad .$$

According to (74), L_{max} can be increased without sacrificing accuracy if $N(E_n, \bar{\Omega}_1)$ can be increased by a constant factor, e.g., by increasing the beam current of an accelerator. Then for a perfect instrument the counting rate is limited only by the existing limitations of source strength. However, as the background rate increases with increasing source intensity, the maximum counting rate is limited in practice by the resolving time of the electronic circuitry associated with the spectrometer.

Calculation of the Minimum Counting Time

The number of counts C taken for one point on a spectrum curve is given by the product of L in (24) and the counting time t. The curve is normally a plot of the experimentally determined values of $N(\bar{E}_n, \bar{\Omega}_1)$ against E_n or Ω_1, as abscissa. In the following discussion only E_n is considered as the abscissa. The coordinate of the point in the ordinate $N(\bar{E}_n, \bar{\Omega}_1)$ is obtained directly from (28) because all terms except $N(\bar{E}_n, \bar{\Omega}_1)$ are specified by the conditions of the experiment. The fractional error in intensity $\frac{\Delta N}{N}$ is determined from the standard deviation as

$$\frac{\Delta N}{N} = \frac{1}{\sqrt{C}} \quad . \tag{75}$$

The fractional error in the ordinate is hereafter denoted by $\sqrt{\overline{\mu^2}}$. The fractional error of a point on the spectrum curve then has two components $\sqrt{\overline{\epsilon^2}}$ along the abscissa, and $\sqrt{\overline{\mu^2}}$ along the ordinate. In order to take cognizance of this fact, let

$$\overline{\delta_1^2} \equiv \overline{\mu^2} + \overline{\epsilon^2} \tag{76}$$

define the total error of a point on the curve.

Since a spectrum curve consists of information about both intensity and energy, it does not appear consistent to measure intensity quite accurately and leave the energy relatively uncertain, or vice versa. For example, it is certainly unsound to provide excellent collimation, but count so few protons as to be unable to make a reasonable estimate of the average rate at which protons traverse the collimator. On the other hand, it appears inefficient to

spend a lot of time taking counts if the collimation is poor. We feel justified therefore in saying that there is an optimum relation between $\overline{\mu^2}$ and $\overline{\epsilon^2}$ which permits the equipment the least time to drift while collecting data for a point with an error $\overline{\delta_1^2}$. This relation is determined by minimizing the counting time subject to (76) being constant, and is the only general consideration we have been able to make which allows for the fact that the equipment is not perfect.

The counting time t, the number of counts C, and the fractional error in the ordinate $\sqrt{\overline{\mu^2}}$ are related by the following equation.

$$C = t\,L = \frac{1}{\overline{\mu^2}} \tag{77}$$

Employing optimum dimensions, (71) becomes

$$\overline{\Delta\rho_{tot}^2} = \overline{\Delta\rho_s^2} + \overline{2\,\Delta\rho_t^2} \quad . \tag{78}$$

Hence

$$\overline{\Delta\rho_t^2} = \frac{\overline{\Delta\rho_{tot}^2} - \overline{\Delta\rho_s^2}}{2} \quad . \tag{79}$$

Substituting (79) into (74) yields

$$L = \frac{1.3\,S}{g}\left(\overline{\Delta\rho_{tot}^2} - \overline{\Delta\rho_s^2}\right)^2 \bar{E}_n\, N(\bar{E}_n, \bar{\Omega}_1)\, \sigma(\bar{E}_n)\, \overline{R} \tag{80}$$

or

$$L = \frac{g^3 S}{12.3}\left(\overline{\epsilon^2} - \overline{\epsilon_s^2}\right)^2 E_n\, N(\bar{E}_n, \bar{\Omega}_1)\, \sigma(\bar{E}_n)\, \overline{R} \tag{81}$$

in terms of the corresponding errors in energy.

The counting time for one point on a spectrum curve is obtained now by inserting (81) into (77).

$$t = \frac{12.3}{g^3 \, s \, \overline{\mu^2} \, (\overline{\epsilon^2} - \overline{\epsilon_s^2})^2 \, \bar{E}_n \, N(\bar{E}_n, \bar{\Omega}_1) \, \sigma(\bar{E}_n)} \, \bar{R} \tag{82}$$

Minimizing t, subject to $\overline{\delta_1^2}$ = constant, yields the relation

$$\overline{\mu^2} = \frac{\overline{\epsilon^2} - \overline{\epsilon_s^2}}{2} , \tag{83}$$

which on the basis of (79) means that $\overline{\mu^2}$ should equal $\overline{\epsilon_t^2}$. Thus the optimum number of counts is given by

$$\left.\begin{aligned} C &= \left(\frac{g}{2}\right)^2 \frac{1}{\overline{\Delta\rho_t^2}} = \frac{3}{2} g^2 \left(\frac{t_o + t_1}{t_1}\right)^2 \\ &= \left(\frac{g}{2}\right)^2 \frac{1}{29.1} \left(\frac{b_2}{a}\right)^4 . \end{aligned}\right\} \tag{84}$$

Substituting (83) into (82) yields

$$t_{min} = \frac{24.6}{g^3 \, s(\overline{\epsilon^2} - \overline{\epsilon_s^2})^3 \, \bar{E}_n \, N(\bar{E}_n, \bar{\Omega}_1) \, \sigma(\bar{E}_n)} \, \bar{R} \tag{85}$$

for the minimum time required to obtain one experimental point subject to $\overline{\delta_1^2} = \overline{\mu^2} + \overline{\epsilon^2}$ = constant. Equation (85) provides a useful feasibility criterion. Suppose there is a need to take measurements in a given range of

intensity values $N(\bar{E}_n, \bar{\Omega}_1)$ and the available time per point is t_{min}. Inserting these values in (85) one can immediately solve for $\overline{\epsilon^2}$ since g, $\overline{\epsilon_s^2}$, and $\sigma(\bar{E}_n)$ are fixed by the choice of $\bar{E}_n$. The value of $\overline{\epsilon^2}$ obtained may be regarded as the practical lower limit of error.

The following equation gives t_{min} in terms of the width at half maximum, which is 2.36 times as great as the r.m.s. error.

$$t_{min} = \frac{4232.2}{g^3 \, S(\overline{\epsilon^2_{hh}} - \overline{\epsilon^2_{hhs}})^3 \, \bar{E}_n \, N(\bar{E}_n, \bar{\Omega}_1) \, \sigma(\bar{E}_n)} \, \bar{R} \tag{86}$$

Since resolution is normally stated in terms of width at half maximum, (86) may be of more practical interest than (85). Equation (86) is plotted in Figs. 6, 7, and 8 for 1.5, 3, and 9 Mev with $N(\bar{E}_n, \bar{\Omega}_1) = 3 \cdot 10^4$ as representative of a plentiful (α,n) source, and $N(\bar{E}_n, \bar{\Omega}_1) = 10^6$ for a fairly copious yield from an accelerator. For isotropic sources the first rate corresponds to a total emission of $3.78 \cdot 10^5$ neutrons/sec/Mev, and the second rate corresponds to $1.26 \cdot 10^7$ neutrons/sec/Mev. Paraffin was selected as a typical radiator, having a hydrogen density of $S = 7.65 \cdot 10^{22}$ atoms/cm^3. The tables of ref. 7 were used for the range data, and values of g were taken from Fig. 2 which is based on the same reference. Adair's[10] compilation was used for the n-p scattering cross sections.

That the data collection time increases with increasing accuracy is to be expected, but the absolute magnitudes here may be surprising to those who have not worked with these instruments. In using the curves it must be kept in mind that they assume perfect discrimination against background. Thus, although a comparison (of the curves in Fig. 6) shows that the data collection time for a point at high energy

UNCLASSIFIED
DWG. 15158A

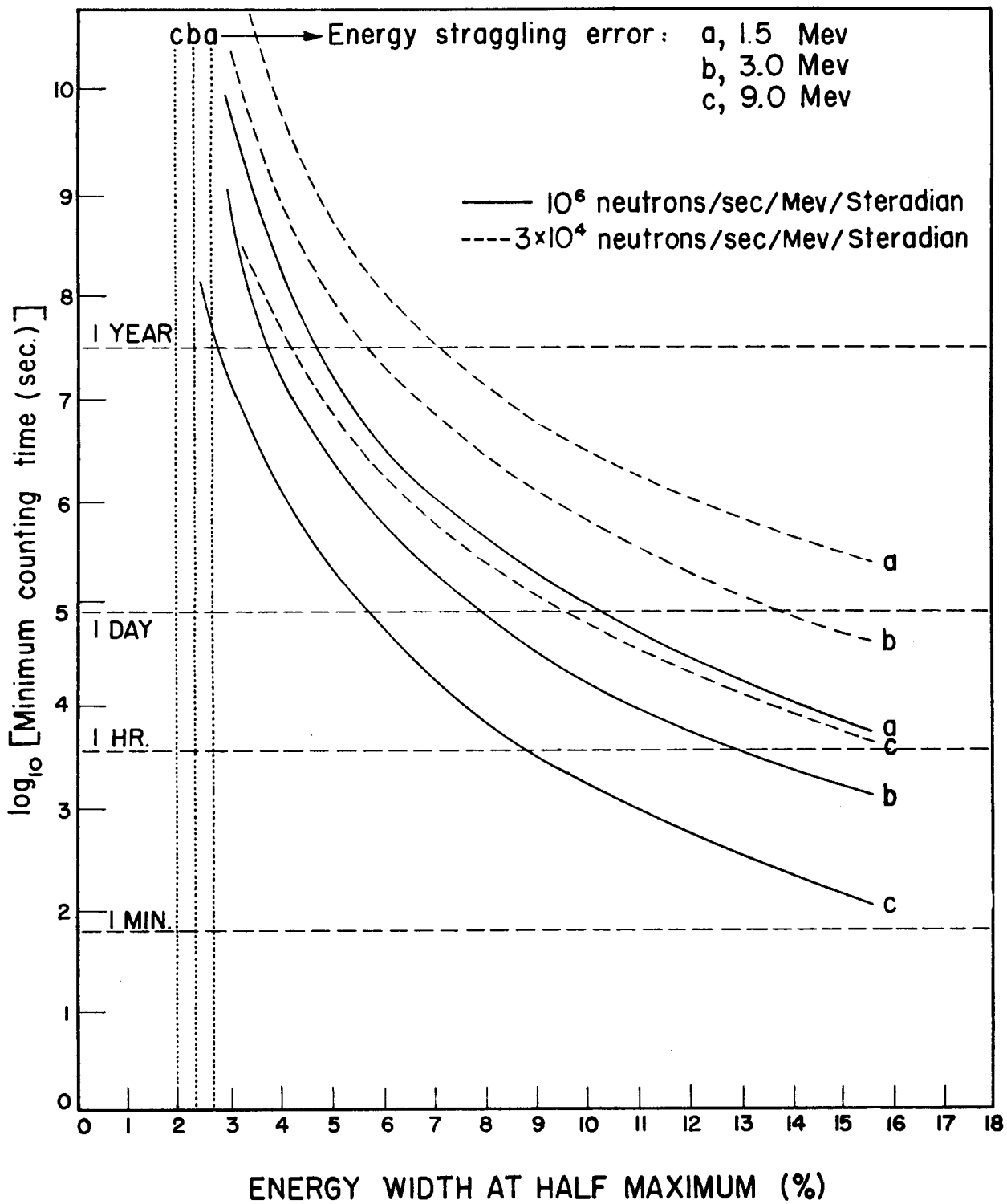

Fig. 6. Graph of Minimum Counting Time vs. Energy Width at Half Maximum.
(Revised)

is less than for a point at low energy, this is not necessarily so in practice because high energy neutrons are capable of producing more background than low energy neutrons. With poor discrimination against background, it takes longer to establish statistical accuracy.

Infinitely Thick Radiator

The thickness of an infinitely thick radiator is greater than the penetration depth of the most energetic recoil protons. Hence it is infinitely thick for protons. At the same time, fast neutrons are so penetrating that the radiator may be regarded as thin in connection with neutron transmission. Thus multiple scattering may be neglected. In treating the thick radiator, we imagine it to be split up into many laminations of equal thickness. The protons of minimum energy, whose range terminates in the detection width, come from the lamination of t_{11} next to t_o, the thickness of absorbing material between the radiator face and the detection width. The contribution of this lamination to the counting rate may be obtained by replacing t_1 by t_{11} in (28).

$$\left.\begin{aligned} dL_1 &= \frac{2\pi S}{g}\left(\frac{a}{b_1}\right)^2\left(\frac{a}{b_2}\right)^2 t_2\,\bar{E}_{n1}\,N(\bar{E}_{n1},\bar{\Omega}_1)\,\sigma(\bar{E}_{n1})\,\frac{t_{11}}{t_o + \frac{t_{11}+t_2}{2}} \\ &= M\,\bar{E}_{n1}\,N(\bar{E}_{n1},\bar{\Omega}_1)\,\sigma(\bar{E}_{n1})\,\frac{t_{11}}{t_o + \frac{t_{11}+t_2}{2}} \end{aligned}\right\} \tag{87}$$

The second lamination faces an absorber of thickness $t_o + t_{11}$ and provides recoils from a radiator of thickness t_{11}. Thus its contribution to the counting rate is

$$dL_2 = M\,\bar{E}_{n2}\,N(\bar{E}_{n2},\bar{\Omega}_1)\,\sigma(\bar{E}_{n2})\,\frac{t_{11}}{t_o + t_{11} + \frac{t_{11}+t_2}{2}} \tag{88}$$

where $\bar{E}_{n2}$ is given by

$$R(\bar{E}_{n2}) = t_o + t_{11} + \frac{t_{11} + t_2}{2} \quad . \tag{89}$$

Similarly, the third and r^{th} contributions are

$$dL_3 = M\,\bar{E}_{n3}\,N(\bar{E}_{n3}, \bar{\Omega}_1)\,\sigma(\bar{E}_{n3}) \quad \frac{t_{11}}{t_o + 2t_{11} + \frac{t_{11} + t_2}{2}} \quad . \tag{90}$$

$$dL_r = M\,\bar{E}_{nr}\,N(\bar{E}_{nr}, \bar{\Omega}_1)\,\sigma(\bar{E}_{nr}) \quad \frac{t_{11}}{t_o + (r-1)\,t_{11} + \frac{t_{11} + t_2}{2}} \quad . \tag{91}$$

Therefore the counting rate for an infinitely thick radiator with absorber t_o is given by the sum

$$L = M \sum_{r=1}^{r_{max}} \frac{\bar{E}_{nr}\,N(\bar{E}_{nr}, \bar{\Omega}_1)\,\sigma(\bar{E}_{nr})\,t_{11}}{t_o + (r-1)\,t_{11} + \frac{t_{11} + t_2}{2}} \tag{92}$$

where

$$r_{max} = \frac{\text{radiator thickness}}{t_{11}} \quad .$$

Since

$$R(\bar{E}_{nr}) = t_o + (r-1)\,t_{11} + \frac{t_{11} + t_2}{2} \quad , \tag{93}$$

the fraction $\dfrac{t_{11}}{t_o + (r-1)\, t_{11} + \dfrac{t_{11} + t_2}{2}}$ in (92) may be replaced by

$\dfrac{\Delta R}{R(\bar{E}_{nr})}$ or $\left(\dfrac{g}{2}\right)\left(\dfrac{\Delta \bar{E}_n}{\bar{E}_{nr}}\right)$ invoking Geiger's Law. Substituting the latter

into (92) yields the following expression for the counting rate

$$L = \pi\, S\, t_2 \left(\frac{a}{b_1}\right)^2 \left(\frac{a}{b_2}\right)^2 \sum_{r=1}^{r_{max}} N(\bar{E}_{nr}, \bar{\Omega}_1)\, \sigma(\bar{E}_{nr})\, \Delta \bar{E}_n \quad . \tag{94}$$

Since there is nothing to prevent us from allowing the number of laminations to increase while $\Delta \bar{E}_n$ correspondingly decreases, we may replace (94) by the limit of the sum.

$$L(\bar{E}_{no}) = \pi\, S\, t_2 \left(\frac{a}{b_1}\right)^2 \left(\frac{a}{b_2}\right)^2 \int_{\bar{E}_{no}}^{\infty} N(\bar{E}_n, \bar{\Omega}_1)\, \sigma(\bar{E}_n)\, d\bar{E}_n \tag{95}$$

where $\bar{E}_{no}$ is given by

$$R(\bar{E}_{no}) = t_o + \frac{t_2}{2} \quad . \tag{96}$$

Consider now that we have a set of experimental values of $L(\bar{E}_{no})$ taken with different absorber thicknesses t_o, and that these values have been plotted against $\bar{E}_{no}$. By taking graphical derivatives of this curve, we obtain values of the function

$$-\frac{dL(\bar{E}_{no})}{d\,\bar{E}_{no}} = \pi\, S\, t_2 \left(\frac{a}{b_1}\right)^2 \left(\frac{a}{b_2}\right)^2 N(\bar{E}_{no}, \bar{\Omega}_1)\, \sigma(\bar{E}_{no}) \quad , \tag{97}$$

which may be solved immediately to obtain $N(\bar{E}_{no}, \bar{\Omega}_1)$.

Except when t_o approaches the range of the most energetic recoils produced by the neutron source, the counting rate is large because it is the sum of the contributions of many laminations in the radiator. Since the counting rate is large, the values of the points $L(\bar{E}_{no})$ are relatively precise. However, the values along the ordinate of the spectrum curve are calculated from the derivative $\frac{dL(\bar{E}_{no})}{d\bar{E}_{no}}$ and hence it is the precision of the derivative which is important. The errors must be indicated on a spectrum curve to provide complete information. If one agrees on this point, he can no longer differentiate the experimental plot of the function $L(\bar{E}_{no})$ in calculating $N(\bar{E}_n, \bar{\Omega}_1)$. Rather, he is forced to take the differences between the experimental points. Otherwise the error given before as $\sqrt{\overline{\mu^2}}$ cannot be evaluated. In taking the difference between two adjacent points where absorber thicknesses are t_o and $t_o + \Delta t_o$, one obtains the contribution to the counting rate from a radiator of Δt_o thickness, and this contribution may be written by (28) as

$$\Delta L_o = M \; \bar{E}_n \; N(\bar{E}_n, \bar{\Omega}_1) \; \sigma(\bar{E}_n) \; \frac{\Delta t_o}{t_o + \frac{\Delta t_o + t_2}{2}} \tag{98}$$

from which the point $N(\bar{E}_n, \bar{\Omega}_1)$ may be immediately obtained. This is the same as would have been obtained directly with a thin radiator of thickness Δt_o and an absorbing length t_o, except for the error $\sqrt{\overline{\mu^2}}$. Consider now the same energy point taken by the two methods where the same number of recoils are observed in each case. Let C and $C_1 - C_2$ denote the number of counts with the thin radiator and the differential number of counts with the thick radiator respectively where $C = C_1 - C_2$. The error with the thin radiator is

$$\sqrt{\overline{\mu^2}} = \frac{1}{\sqrt{C}} = \frac{1}{\sqrt{C_1 - C_2}} \tag{99}$$

while the error with the thick radiator is

$$\sqrt{\overline{\mu^2}} = \frac{\sqrt{C_1 + C_2}}{C_1 - C_2} \quad .$$

Thus the error with the thick radiator is greater because it is $\sqrt{\frac{C_1 + C_2}{C_1 - C_2}}$ times as great. Then the only difference between the thin and thick radiator is that the latter provides poorer statistics in spite of a higher apparent counting rate.

In case the spectrum consists of several widely spaced lines, a thick radiator may be used conveniently to locate the lines. With one line, the intensity may be represented by $N(E_n, \bar{\Omega}_1)\ \delta(\bar{E}_{no} - \bar{E}_n)$, where $\delta(\bar{E}_{no} - \bar{E}_n)$ is the delta function. Here

$$\left.\begin{aligned} L(\bar{E}_{no}) &= \pi\ S\ t_2 \left(\frac{a}{b_1}\right)^2 \left(\frac{a}{b_2}\right)^2 N(E_n, \bar{\Omega}_1)\sigma(E_n) \quad \text{for} \quad \bar{E}_{no} \angle E_n \\ &= 0 \qquad\qquad\qquad\qquad\qquad\qquad\qquad\qquad \text{for} \quad E_n \angle \bar{E}_{no} \end{aligned}\right\} \tag{100}$$

For two lines

$$\left.\begin{aligned} L(\bar{E}_{no}) &= \pi\, S\, t_2 \left(\frac{a}{b_1}\right)^2 \left(\frac{a}{b_2}\right)^2 \left[N(E_{n1}, \bar{\Omega}_1)\sigma(E_{n1}) + N(E_{n2}, \bar{\Omega}_1)\sigma(E_{n2})\right] && \text{for } \bar{E}_{no} \angle E_{n1} \angle E_{n2} \\ &= \pi\, S\, t_2 \left(\frac{a}{b_1}\right)^2 \left(\frac{a}{b_2}\right)^2 \left[N(E_{n2}, \bar{\Omega}_1)\sigma(E_{n2})\right] && \text{for } E_{n1} \angle \bar{E}_{no} \angle E_{n2} \\ &= 0 && \text{for } E_{n2} \angle \bar{E}_{no} \end{aligned}\right\} \quad (101$$

The extension to n lines is clear from the above.

Acknowledgments

The above calculations are an outgrowth of experimental work done at Oak Ridge in collaboration with Mr. Keith Henry in the interval 1948 - 1950. The writer resumed this work as a consultant to Oak Ridge National Laboratory in 1951. During all this time the writer has enjoyed many stimulating discussions with various people on these problems. Among those to whom he is in particular debt for valuable counsel and material support are Dr. K. Lark-Horovitz, department head, and Dr. E. Bleuler at Purdue University; Dr. J. L. Meem, Mr. R. G. Cochran, and Mr. K. Henry at Oak Ridge National Laboratory; Dr. Clark Goodman at M.I.T.; and Dr. C. E. Mandeville at Bartol Research Foundation.

References

1. Watt, B. E., Energy Spectrum of Neutrons from Fission Induced by Thermal Neutrons, AECD-3073.

2. Hill, D. L., Studies with the Ranger, AECD-1945.

3. Kinsey, B. B., S. G. Cohen, and J. Dainty, "A Coincidence Method of Measuring a Flux of Fast Neutrons", Camb. Phil. Soc. Proc. 44, (1948), pp 96 - 113.

4. Cohen, B. L., and C. E. Falk, "(d,n) Reactions with 15 Mev Deuterons II Neutron Energy Spectra and Yields", Phys. Rev. 84, (1951), pp 173 - 178.

5. Gossick, B. R., and K. Henry, "Neutron Energy Spectrometer", ORNL-711, June 6, 1950.

6. Segrè, E., "Scattering of Nuclear Particles and Nuclear Forces", Proc. International Conference in Nuclear Physics and the Physics of Fundamental Particles, September 17 - 22, 1951.

7. Hirschfelder, J. O., and J. L. Magee, "Range-Energy Relations for Protons in Substances Containing C, H, O, A, and Xe", Phys. Rev. 73, (1948), pp 207 - 215.

8. Livingston, M. Stanley, and H. A. Bethe, "Nuclear Dynamics, Experimental", Rev. Mod. Phys. (1937).

9. Bethe, H. A., "The Properties of Atomic Nuclei, II Range-Energy Curves", BNL-T-7.

10. Adair, R. K., "Neutron Cross Sections of the Elements", Rev. Mod. Phys. 22, (1950), p 249.

Appendix 1

The x', y', z' coordinates (Fig. 4) are transformed into the $x^{1\prime}$, $y^{1\prime}$, $z^{1\prime}$ coordinates by the equation

$$\begin{pmatrix} x^1 \\ y^1 \\ z^1 \end{pmatrix} = \begin{pmatrix} \cos\lambda & 0 & -\sin\lambda \\ 0 & 1 & 0 \\ \sin\lambda & 0 & \cos\lambda \end{pmatrix} \begin{pmatrix} x \\ y \\ z \end{pmatrix}, \tag{a1.1}$$

which with good geometry may be approximated by

$$\begin{pmatrix} x^1 \\ y^1 \\ z^1 \end{pmatrix} = \begin{pmatrix} 1 & 0 & -\lambda \\ 0 & 1 & 0 \\ \lambda & 0 & 1 \end{pmatrix} \begin{pmatrix} x \\ y \\ z \end{pmatrix} \tag{a2.1}$$

In turn, the $x^{1\prime}$, $y^{1\prime}$, $z^{1\prime}$ coordinates may be transformed into $\overline{PR}, \psi, \varphi$ coordinates by the equation

$$\begin{pmatrix} x^1 \\ y^1 \\ z^1 \end{pmatrix} = \overline{PR} \begin{pmatrix} \sin\psi \cos\varphi \\ \sin\psi \sin\varphi \\ \cos\psi \end{pmatrix} \tag{a3.1}$$

The coordinates of the point at the terminus of $\overline{PR}$ in the x', y', z' system are $\left[x - b_1 \lambda, y, b_2\right]$. Placing these in (a1.1) obtains the coordinates of the same point in the $x^{1\prime}$, $y^{1\prime}$, $z^{1\prime}$ system, namely the point

$$\left[x - (b_1 + b_2)\lambda, y, x\lambda - b_1\lambda^2 + b_2\right] . \tag{a4.1}$$

Thus, we may write

$$\sin\psi = \frac{\sqrt{\left[x - (b_1 + b_2)\lambda\right]^2 + y^2}}{\overline{PR}} , \tag{a5.1}$$

$$\cos\psi = \frac{x\lambda - b_1\lambda^2 + b_2}{\overline{PR}} . \tag{a6.1}$$

By (a3.1), (a4.1) and (a5.1) it follows that

$$\cos\varphi = \frac{x - (b_1 + b_2)\lambda}{\sqrt{\left[x - (b_1 + b_2)\lambda\right]^2 + y^2}} , \tag{a7.1}$$

$$\sin\varphi = \frac{y}{\sqrt{\left[x - (b_1 + b_2)\lambda\right]^2 + y^2}} . \tag{a8.1}$$

Making the substitutions indicated by (17), (18), (19), and (20) of the main text and by differentiating (a4.1) through (a8.1), the following may be obtained:

$$\frac{\partial\varphi}{\partial\eta} = \frac{\xi - (1 + \delta)\lambda}{\left[\xi - (1 + \delta)\lambda\right]^2 + \eta^2} \tag{a9.1}$$

$$\frac{\partial\varphi}{\partial\xi} = \frac{-\eta}{\left[\xi - (1 + \delta)\lambda\right]^2 + \eta^2} \tag{a10.1}$$

$$\frac{\partial\psi}{\partial\eta} = \frac{\eta(\xi\lambda - \delta\lambda^2 + 1)}{\sqrt{[\xi - (1+\delta)\lambda]^2 + \eta^2}\,\left[(\xi - \delta\lambda)^2 + \eta^2 + 1\right]} \qquad \text{(a11.1)}$$

$$\frac{\partial\psi}{\partial\xi} = \frac{(\xi - \delta\lambda) - (\eta^2 + 1)\lambda}{\sqrt{[\xi - (1+\delta)\lambda]^2 + \eta^2}\,\left[(\xi - \delta\lambda)^2 + \eta^2 + 1\right]} \qquad \text{(a12.1)}$$

By forming the Jacobian with (a9.1) through (a12.1) and applying the factor $\sin\psi\cos\psi$, the following is obtained:

$$\sin\psi\cos\psi\,|J| =$$

$$\frac{\{\xi\lambda - \delta\lambda^2 + 1\}\;\{[\xi - (1+\delta)\lambda]^2 + \eta^2 + \eta^2\lambda^2\}}{\{(\xi - \delta\lambda)^2 + \eta^2 + 1\}^2\;\{[\xi - (1+\delta)\lambda]^2 + \eta^2\}} \qquad \text{(a13.1)}$$

Neglecting terms of order ξ^2, which is permissable with "good geometry," (a13.1) equals unity.

Appendix 2

$$I_1 = \int_0^{a/b_1} \int_{-\alpha}^{\alpha} \int_{-\sqrt{\alpha^2-\eta^2}}^{\sqrt{\alpha^2-\eta^2}} \lambda \, d\xi \, d\eta \, d\lambda \tag{A1.2}$$

$$= 2 \int_0^{a/b_1} \int_{-\alpha}^{\alpha} \lambda \sqrt{\alpha^2 - \eta^2} \, d\eta \, d\lambda \tag{A2.2}$$

$$\int_{-\alpha}^{\alpha} \sqrt{\alpha^2 - \eta^2} \, d\eta = \frac{\pi\alpha^2}{2} \tag{A3.2}$$

$$I_1 = \pi \alpha^2 \int_0^{a/b_1} \lambda \, d\lambda = \frac{\pi\alpha^2}{2} \left(\frac{a}{b_1}\right)^2 \tag{A4.2}$$

Appendix 3

$$\overline{\rho_{ac}} = \frac{g}{2} A_a \int_0^{a/b_1} \int_{-\alpha}^{\alpha} \int_{-\sqrt{\alpha^2-\eta^2}}^{\sqrt{\alpha^2-\eta^2}} \left\{ \xi^2 + \left[(1+\delta)\lambda - \eta \right]^2 \right\} \lambda \, d\xi \, d\eta \, d\lambda \quad \text{(A1.3)}$$

$$\overline{\rho_{ao}} = \frac{1}{2} A_a \int_0^{a/b_1} \int_{-\alpha}^{\alpha} \int_{-\sqrt{\alpha^2-\eta^2}}^{\sqrt{\alpha^2-\eta^2}} \left[\xi^2 + (\delta\lambda - \eta)^2 \right] \lambda \, d\xi \, d\eta \, d\lambda \quad \text{(A2.3)}$$

Let

$$J_1 = \int_0^{a/b_1} \int_{-\alpha}^{\alpha} \int_{-\sqrt{\alpha^2-\eta^2}}^{\sqrt{\alpha^2-\eta^2}} \lambda \xi^2 \, d\xi \, d\eta \, d\lambda \quad \text{(A3.3)}$$

and

$$J_2 = \int_0^{a/b_1} \int_{-\alpha}^{\alpha} \int_{-\sqrt{\alpha^2-\eta^2}}^{\sqrt{\alpha^2-\eta^2}} \lambda (k\lambda - \eta)^2 \, d\xi \, d\eta \, d\lambda \quad . \quad \text{(A4.3)}$$

$$J_1 = \frac{2}{3} \int_0^{a/b_1} \int_{-\alpha}^{\alpha} \lambda (\alpha^2 - \eta^2)^{3/2} \, d\eta \, d\lambda \quad . \quad \text{(A5.3)}$$

Let

$$(\alpha^2 - \eta^2)^{1/2} = \alpha \sin \theta_1 \quad . \quad \text{(A6.3)}$$

Then

$$\eta = \alpha \cos \theta_1 \quad \text{(A7.3)}$$

and

$$d\eta = -\alpha \sin \theta_1 \, d\theta_1 \quad . \quad \text{(A8.3)}$$

$$\int_{-\alpha}^{\alpha} (\alpha^2 - \eta^2)^{3/2} \, d\eta = - \int_{\pi}^{0} (\alpha \sin \theta_1)^{S+1} \, d\theta_1 \tag{A9.3}$$

$$= \alpha^{S+1} \int_{0}^{\pi} (\sin \theta_1)^{S+1} \, d\theta_1 \tag{A10.3}$$

$$= \frac{S \, \alpha^{S+1}}{S+1} \int_{0}^{\pi} (\sin \theta_1)^{S-1} \, d\theta_1 \quad . \tag{A11.3}$$

Furthermore

$$\int_{0}^{\pi} (\sin \theta_1)^2 \, d\theta_1 = \left[\frac{\theta_1}{2} - \frac{\sin 2 \, \theta_1}{4} \right]_{0}^{\pi} = \frac{\pi}{2} \quad . \tag{A12.3}$$

Thus

$$J_1 = \frac{\alpha^4}{2} \int_{0}^{a/b_1} \lambda \, d\lambda \int_{0}^{\pi} (\sin \theta_1)^2 \, d\theta_1 \tag{A13.3}$$

$$= \frac{\pi}{8} \alpha^4 \left(\frac{a}{b_1} \right)^2 \quad . \tag{A14.3}$$

$$J_2 = 2 \int_{0}^{a/b_1} \int_{-\alpha}^{\alpha} \lambda (k \lambda - \eta)^2 (\alpha^2 - \eta^2)^{1/2} \, d\eta \, d\lambda \tag{A15.3}$$

$$= 2 \int_{0}^{a/b_1} \int_{-\alpha}^{\alpha} \left[k^2 \lambda^3 - 2k\eta\lambda + \lambda \eta^2 \right] (\alpha^2 - \eta^2)^{1/2} \, d\eta \, d\lambda \tag{A16.3}$$

$$= J_{21} + J_{22} + J_{23} \quad . \tag{A17.3}$$

By (A3.2)

$$J_{21} = 2\,k^2 \int_0^{a/b_1} \lambda^3\, d\lambda \; \frac{\pi\,\alpha^2}{2} \tag{A18.3}$$

$$= \frac{\pi\,k^2}{4}\,\alpha^2 \left(\frac{a}{b_1}\right)^4 . \tag{A19.3}$$

Since it is an odd function in η

$$J_{22} = 0 . \tag{A20.3}$$

$$J_{23} = 2 \int_0^{a/b_1} \int_{-\alpha}^{\alpha} \lambda\eta^2 (\alpha^2 - \eta^2)^{1/2}\, d\eta\, d\lambda . \tag{A21.3}$$

$$\int_{-\alpha}^{\alpha} \eta^2(\alpha^2 - \eta^2)^{1/2}\, d\eta = \alpha^4 \int_0^{\pi} (\cos\theta_1)^2 (\sin\theta_1)^2\, d\theta_1 \tag{A22.3}$$

$$= \alpha^4 \int_0^{\pi} \left[(\sin\theta_1)^2 - (\sin\theta_1)^4\right] d\theta_1 . \tag{A23.3}$$

As $$\int_0^{\pi} (\sin\theta_1)^4\, d\theta_1 = \frac{3}{4} \int_0^{\pi} (\sin\theta_1)^2\, d\theta_1 \tag{A24.3}$$

$$\int_{-\alpha}^{\alpha} \eta^2 (\alpha^2 - \eta^2)^{1/2}\, d\eta = \frac{\alpha^4}{4} \int_0^{\pi} (\sin\theta_1)^2\, d\theta_1 = \frac{\pi}{8}\,\alpha^4 . \tag{A25.3}$$

$$J_{23} = \frac{\pi}{4}\,\alpha^4 \int_0^{a/b_1} \lambda\, d\lambda = \frac{\pi}{8}\,\alpha^4 \left(\frac{a}{b_1}\right)^2 . \tag{A26.3}$$

$$J_2 = J_{21} + J_{23} = \frac{\pi}{4} \left(\frac{a}{b_1}\right)^2 \alpha^2 \left[k^2 \left(\frac{a}{b_1}\right)^2 + \frac{\alpha^2}{2}\right] . \tag{A27.3}$$

$$\overline{\rho_{ac}} = \frac{g}{2} A_a \left\{ J_1 + J_2 \right\} \quad \text{for} \quad k = (1 + \delta) \ . \tag{A28.3}$$

$$\overline{\rho_{ao}} = \frac{1}{2} A_a \left\{ J_1 + J_2 \right\} \quad \text{for} \quad k = \delta \ . \tag{A29.3}$$

Thus all terms in $\overline{\rho_a}$ have been evaluated.

Appendix 4

$$\overline{\rho_a^2} = \overline{\rho_{ac}^2} + 2\,\overline{\rho_{ao}\,\rho_{ac}} + \overline{\rho_{ao}^2} \quad , \tag{A1.4}$$

$$\rho_{ac}^2 = \frac{g^2}{4}\left\{\xi^4 + 2\left[(1+\delta)\,\lambda - \eta\right]^2 \xi^2 + \left[(1+\delta)\,\lambda - \eta\right]^4\right\} , \tag{A2.4}$$

$$2\,\rho_{ao}\,\rho_{ac} = \frac{g}{2}\left\{\xi^4 + \left(\left[\delta\lambda - \eta\right]^2 + \left[(1+\delta)\,\lambda - \eta\right]^2\right)\xi^2 + (\delta\lambda - \eta)^2\left[(1+\delta)\,\lambda - \eta\right]^2\right\} , \tag{A3.4}$$

$$\rho_{ao}^2 = \frac{1}{4}\left\{\xi^4 + 2(\delta\lambda - \eta)^2\,\xi^2 + (\delta\lambda - \eta)^4\right\} . \tag{A4.4}$$

Let

$$T_1 = \int_0^{a/b_1}\int_{-\alpha}^{\alpha}\int_{-\sqrt{\alpha^2-\eta^2}}^{\sqrt{\alpha^2-\eta^2}} \xi^4\lambda \; d\xi \; d\eta \; d\lambda \quad , \tag{A5.4}$$

$$T_2 = \int_0^{a/b_1}\int_{-\alpha}^{\alpha}\int_{-\sqrt{\alpha^2-\eta^2}}^{\sqrt{\alpha^2-\eta^2}} (k_2\lambda - \eta)^2\,\xi^2\lambda \; d\xi \; d\eta \; d\lambda \, , \tag{A6.4}$$

$$T_3 = \int_0^{a/b_1}\int_{-\alpha}^{\alpha}\int_{-\sqrt{\alpha^2-\eta^2}}^{\sqrt{\alpha^2-\eta^2}} (k_2\lambda - \eta)^4\lambda \; d\xi \; d\eta \; d\lambda \quad , \tag{A7.4}$$

$$T_4 = \int_0^{a/b_1}\int_{-\alpha}^{\alpha}\int_{-\sqrt{\alpha^2-\eta^2}}^{\sqrt{\alpha^2-\eta^2}} (k_1\lambda - \eta)^2\,(k_2\lambda - \eta)^2\lambda \; d\xi \; d\eta \; d\lambda \tag{A8.4}$$

$$T_1 = \frac{2}{5} \int_0^{a/b_1} \int_{-\alpha}^{\alpha} (\alpha^2 - \eta^2)^{5/2} \lambda \, d\eta \, d\lambda \tag{A9.4}$$

$$= \frac{1}{5} \left(\frac{a}{b_1}\right)^2 \int_{-\alpha}^{\alpha} (\alpha^2 - \eta^2)^{5/2} \, d\eta \, . \tag{A10.4}$$

By Eq. (A11.3)

$$T_1 = \left(\frac{a}{b_1}\right)^2 \frac{\alpha^6}{6} \int_0^{\pi} (\sin \theta_1)^4 \, d\theta_1 = \left(\frac{a}{b_1}\right)^2 \frac{\alpha^6}{8} \int_0^{\pi} (\sin \theta_1)^2 \, d\theta_1 \tag{A11.4}$$

$$= \frac{\pi}{16} \left(\frac{a}{b_1}\right)^2 \alpha^6 \, , \tag{A12.4}$$

$$T_2 = \frac{2}{3} \int_0^{a/b_1} \int_{-\alpha}^{\alpha} (k_2 \lambda - \eta)^2 (\alpha^2 - \eta^2)^{3/2} \lambda \, d\eta \, d\lambda \tag{A13.4}$$

$$= \frac{2}{3} \int_0^{a/b_1} \int_{-\alpha}^{\alpha} (k_2^2 \lambda^3 - 2k_2 \lambda^2 \eta + \eta^2 \lambda)(\alpha^2 - \eta^2)^{3/2} \, d\eta \, d\lambda \, . \tag{A14.4}$$

Since $\eta(\alpha^2 - \eta^2)^{3/2}$ is an odd function in η, the second term drops out.

$$T_2 = \frac{2}{3} \int_0^{a/b_1} \int_{-\alpha}^{\alpha} (k_2^2 \lambda^3 + \eta^2 \lambda)(\alpha^2 - \eta^2)^{3/2} \, d\eta \, d\lambda \tag{A15.4}$$

$$= T_{21} + T_{22} \, . \tag{A16.4}$$

$$T_{21} = \frac{2}{3} \int_0^{a/b_1} \int_{-\alpha}^{\alpha} k_2^2 \lambda^3 (\alpha^2 - \eta^2)^{3/2} \, d\eta \, d\lambda \tag{A17.4}$$

$$= \frac{k_2^2}{6} \left(\frac{a}{b_1}\right)^4 \int_{-\alpha}^{\alpha} (\alpha^2 - \eta^2)^{3/2} \, d\eta \, d\lambda \ . \tag{A18.4}$$

By Eqs. (A11.3) and (A12.3),

$$T_{21} = \frac{\pi}{16} k_2^2 \left(\frac{a}{b_1}\right)^4 \alpha^4 \tag{A19.4}$$

$$T_{22} = \frac{2}{3} \int_0^{a/b_1} \int_{-\alpha}^{\alpha} \eta^2 \lambda (\alpha^2 - \eta^2)^{3/2} \, d\eta \, d\lambda \tag{A20.4}$$

$$= \frac{1}{3} \left(\frac{a}{b_1}\right)^2 \int_{-\alpha}^{\alpha} \eta^2 (\alpha^2 - \eta^2)^{3/2} \, d\eta \ . \tag{A21.4}$$

By Eqs. (A6.3), (A7.3), and (A8.3),

$$T_{22} = \frac{1}{3} \left(\frac{a}{b_1}\right)^2 \alpha^6 \int_0^{\pi} (\cos \theta_1)^2 (\sin \theta_1)^4 \, d\theta_1 \tag{A22.4}$$

$$= \frac{1}{3} \left(\frac{a}{b_1}\right)^2 \alpha^6 \int_0^{\pi} \left[(\sin \theta_1)^4 - (\sin \theta_1)^6\right] d\theta_1 \ . \tag{A23.4}$$

By Eqs. (A11.3) and (A12.3), the definite integral above equals $\frac{\pi}{16}$.

$$T_{22} = \frac{\pi}{48} \left(\frac{a}{b_1}\right)^2 \alpha^6 \ . \tag{A24.4}$$

$$T_2 = \frac{\pi}{16} k_2^2 \left(\frac{a}{b_1}\right)^4 \alpha^4 + \frac{\pi}{48} \left(\frac{a}{b_1}\right)^2 \alpha^6 . \tag{A25.4}$$

To evaluate T_3 we first expand $(k_2 \lambda - \eta)^4$ and omit odd terms in η, since they contribute nothing to the integral. In this manner T_3 becomes

$$T_3 = \int_0^{a/b_1} \int_{-\alpha}^{\alpha} \int_{-\sqrt{\alpha^2 - \eta^2}}^{\sqrt{\alpha^2 - \eta^2}} (k_2^4 \lambda^5 + 6k_2^2 \lambda^3 \eta^2 + \lambda \eta^4) \, d\xi \, d\eta \, d\lambda \tag{A26.4}$$

$$= T_{31} + T_{32} + T_{33} . \tag{A27.4}$$

$$T_{31} = 2k_2^4 \int_0^{a/b_1} \int_{-\alpha}^{\alpha} \lambda^5 \sqrt{\alpha^2 - \eta^2} \, d\eta \, d\lambda \tag{A28.4}$$

$$= \frac{k_2^4}{3} \left(\frac{a}{b_1}\right)^6 \int_{-\alpha}^{\alpha} \sqrt{\alpha^2 - \eta^2} \, d\eta . \tag{A29.4}$$

By Eq. (A3.2)

$$T_{31} = \frac{\pi}{6} k_2^4 \alpha^2 \left(\frac{a}{b_1}\right)^6 , \tag{A30.4}$$

$$T_{32} = 6k_2^2 \int_0^{a/b_1} \int_{-\alpha}^{\alpha} \int_{-\sqrt{\alpha^2 - \eta^2}}^{\sqrt{\alpha^2 - \eta^2}} \lambda^3 \eta^2 \, d\xi \, d\eta \, d\lambda \tag{A31.4}$$

$$= 12k_2^2 \int_0^{a/b_1} \int_{-\alpha}^{\alpha} \lambda^3 \eta^2 \sqrt{\alpha^2 - \eta^2} \, d\eta \, d\lambda \tag{A32.4}$$

$$= 3k_2^2 \left(\frac{a}{b_1}\right)^4 \int_{-\alpha}^{\alpha} \eta^2 \sqrt{\alpha^2 - \eta^2}\, d\eta\, d\lambda \quad . \tag{A33.4}$$

By Eq. (A25.3)

$$T_{32} = \frac{3\pi}{8} k_2^2 \left(\frac{a}{b_1}\right)^4 \alpha^4 \quad , \tag{A34.4}$$

$$T_{33} = 2 \int_0^{a/b_1} \int_{-\alpha}^{\alpha} \lambda \eta^4 \sqrt{\alpha^2 - \eta^2}\, d\eta\, d\lambda \quad . \tag{A35.4}$$

$$= \left(\frac{a}{b_1}\right)^2 \int_{-\alpha}^{\alpha} \eta^4 \sqrt{\alpha^2 - \eta^2}\, d\eta \quad . \tag{A36.4}$$

By the transformation indicated in Eq. (A6.3), the equation for T_{33} may be written as

$$T_{33} = \left(\frac{a}{b_1}\right)^2 \alpha^6 \int_0^{\pi} (\sin \theta_1)^2 (\cos \theta_1)^4 \, d\theta_1 \tag{A37.4}$$

$$= \left(\frac{a}{b_1}\right)^2 \alpha^6 \int_0^{\pi} \left[(\sin \theta_1)^2 - 2(\sin \theta_1)^4 + (\sin \theta_1)^6\right] d\theta_1 \quad . \tag{A38.4}$$

By Eqs. (A11.3) and (A12.3)

$$T_{33} = \left(\frac{a}{b_1}\right)^2 \alpha^6 \left[\frac{\pi}{2} - \frac{3\pi}{4} + \frac{5\pi}{16}\right] = \frac{\pi}{16} \left(\frac{a}{b_1}\right)^2 \alpha^6 \quad , \tag{A39.4}$$

$$T_3 = \frac{\pi}{6} k_2^4 \left(\frac{a}{b_1}\right)^6 \alpha^2 + \frac{3\pi}{8} k_2^2 \left(\frac{a}{b_1}\right)^4 \alpha^4 + \frac{\pi}{16} \left(\frac{a}{b_1}\right)^2 \alpha^6 \quad . \tag{A40.4}$$

In order to treat T_4, we expand the product $(k_1 \lambda - \eta)^2 (k_2 \lambda - \eta)^2$ and omit odd terms in η .

$$T_4 = \int_0^{a/b_1} \int_{-\alpha}^{\alpha} \int_{-\sqrt{\alpha^2 - \eta^2}}^{\sqrt{\alpha^2 - \eta^2}} (k_3 \lambda^5 + k_4 \lambda^3 \eta^2 + \lambda \eta^4) \, d\xi \, d\eta \, d\lambda \quad , \tag{A41.4}$$

where

$$k_3 = (k_1 k_2)^2 \quad , \tag{A42.4}$$

$$k_4 = (k_1^2 + 4k_1 k_2 + k_2^2) \quad . \tag{A43.4}$$

By Eq. (A26.4)

$$T_4 = \frac{k_3}{k_2^4} T_{31} + \frac{k_4}{6k_2^2} T_{32} + T_{33} \tag{A44.4}$$

$$= \frac{\pi}{6} k_3 \alpha^2 \left(\frac{a}{b_1}\right)^6 + \frac{\pi}{16} k_4 \left(\frac{a}{b_1}\right)^4 \alpha^4 + \frac{\pi}{16} \left(\frac{a}{b_1}\right)^2 \alpha^6 \tag{A45.4}$$

$$= \frac{\pi}{6} (k_1 k_2 \alpha)^2 \left(\frac{a}{b_1}\right)^6 + \frac{\pi}{16} (k_1^2 + 4k_1 k_2 + k_2^2) \left(\frac{a}{b_1}\right)^4 \alpha^4 + \frac{\pi}{16} \left(\frac{a}{b_1}\right)^2 \alpha^6 \quad . \tag{A46.4}$$

By Eq. (A2.4)

$$\overline{\rho_{ac}^2} = \frac{g^2}{4} A_a (T_1 + 2T_2 + T_3) \qquad \text{for } k_2 = (\delta + 1) \quad . \tag{A47.4}$$

By Eq. (A3.4)

$$2\,\overline{\rho_{ao}\,\rho_{ac}} = \frac{g}{2}\,A_a \left\{ \underset{k_2 = \delta}{T_1} + \underset{k_2 = (\delta + 1)}{T_2} + \underset{\substack{k_1 = \delta \\ k_2 = (\delta + 1)}}{T_2 + T_4} \right\} \tag{A48.4}$$

By Eq. (A4.4)

$$\overline{\rho_{ao}^{2}} = \frac{1}{4}\,A_a\,(T_1 + 2T_2 + T_3) \quad \text{for } k_2 = \delta\,. \tag{A49.4}$$

$\overline{\rho_a^2}$ is the sum of Eqs. (A47.4), (A48.4), and (A49.4). $\overline{\rho_a}$ was evaluated in Appendix 3. Then $\Delta\overline{\rho_a^2} = \overline{\rho_a^2} - \left(\overline{\rho_a}\right)^2$ has been evaluated, except for the elementary process of squaring $\overline{\rho_a}$ and collecting terms which have been omitted to save space. The result is given as Eq. (54) of the main test. Equation (54) may also be written in the form:

$$\overline{\Delta\rho_a^2} = \frac{g^2}{48}\left(\frac{a}{b_1}\right)^4 + \frac{g^2}{12}\left(\frac{a}{b_1}\right)^3\left(\frac{a}{b_2}\right) + \frac{g(6g+1)}{24}\left(\frac{a}{b_1}\right)^2\left(\frac{a}{b_2}\right)^2$$

$$+ \frac{g(g+1)}{3}\left(\frac{a}{b_1}\right)\left(\frac{a}{b_2}\right)^3 + \frac{(g+1)^2}{6}\left(\frac{a}{b_2}\right)^4 . \tag{A50.4}$$

Appendix 5

Let

$$\frac{1}{b_1} = \beta_1 \quad , \tag{A1.5}$$

$$\frac{1}{b_2} = \beta_2 \quad , \tag{A2.5}$$

$$\beta_1 = \beta_2(2 + \Delta) \quad . \tag{A3.5}$$

Making the substitutions indicated above in Eq. (54) of the main text, and neglecting all terms in Δ^2 and of higher order, one obtains

$$\overline{\Delta \rho_a^2} = \beta_2^4 \left[q + 9(1 + \frac{2\Delta}{3})q_2 + 81(1 + \frac{4\Delta}{3})q_3 + 3q_4 + 4q_4 \right] , \tag{A4.5}$$

where the q's are given by Eqs. (58) through (61) of the main text.

$$\overline{\Delta \rho_a^2} = (K_A + K_B \Delta)\beta_2^4 \quad . \tag{A5.5}$$

$$d\,\overline{\Delta \rho_a^2} = \beta_2^4 K_B \, d\Delta + 4\beta_2^3 (K_A + K_B \Delta) d\beta_2 \quad . \tag{A6.5}$$

By Eqs. (28), (A1.5), and (A2.5) the counting rate may be written here as

$$L = K_C \beta_1^2 \beta_2^2 = K_C \beta_2^4 4(1 + \frac{\Delta}{2})^2 \quad . \tag{A7.5}$$

$$dL = 4K_C (1 + \frac{\Delta}{2})\beta_2^3 \left[\beta_2 d\Delta + 4(1 + \frac{\Delta}{2}) d\beta_2 \right] \quad . \tag{A8.5}$$

We now maximize Eq. (A7.5) subject to Eq. (A5.5) being constant. Let α' be a Lagrangian multiplier.

$$4K_C(1 + \frac{\Delta}{2})\beta_2^4 + \alpha' \beta_2 K_B = 0 \tag{A9.5}$$

$$16K_C(1 + \frac{\Delta}{2})^2 \beta_2^3 + 4\alpha'(K_A + K_B \Delta) = 0 \tag{A10.5}$$

By Eq. (A9.5)

$$\alpha' = \frac{- 4K_C(1 + \frac{\Delta}{2})\beta_2^3}{K_B} \tag{A11.5}$$

Substituting Eq. (A11.5) into Eq. (A10.5) and collecting terms, yields

$$\Delta = 2(1 - \frac{K_A}{K_B}) , \tag{A12.5}$$

$$2 + \Delta = 2(2 - \frac{K_A}{K_B}) . \tag{A13.5}$$

Then by Eq. (A3.5)

$$\beta_1 = 2(2 - \frac{K_A}{K_B})\beta_2 \tag{A14.5}$$

or

$$\frac{b_2}{b_1} = 2(2 - \frac{K_A}{K_B}) . \tag{A15.5}$$

By Eqs. (A4.5) and (A5.5)

$$K_A = q_1 + 9q_2 + 81q_3 + 3q_4 \quad , \tag{A16.5}$$

$$K_B = 4q_2 + 108q_3 + q_4 \quad . \tag{A17.5}$$

Appendix 6

By Eq. (36)

$$\overline{\Delta \rho_t^2} = A_t \int_{-\infty}^{\infty} \rho_t^2 \; t(r)dr \quad , \tag{A1.6}$$

$$\left.\begin{aligned} t(r) &= t_1 \\ &= t_1 \quad \text{for } 0 < |r| < \frac{t_2 - t_1}{2} \\ &= -r + \frac{t_1 + t_2}{2} \quad \text{for } \frac{t_2 - t_1}{2} < |r| < \frac{t_1 + t_2}{2} \\ &= 0 \quad \text{for } \frac{t_1 + t_2}{2} < |r| \, , \end{aligned}\right\} \tag{35}$$

$$\rho_t(r) = \frac{r}{\bar{R}} \quad . \tag{64}$$

By Eqs. (35) and (64) it may be seen that $\rho_t^2 \, t(r)$ is an even function in r. Hence,

$$\overline{\Delta \rho_t^2} = 2 \, A_t \int_0^{\infty} \rho_t^2 \, t(r)dr \tag{A2.6}$$

$$= \frac{2A_t}{(\bar{R})^2} \left\{ t_1 \int_0^{\frac{t_2 - t_1}{2}} r^2 dr + \int_{\frac{t_2 - t_1}{2}}^{\frac{t_1 + t_2}{2}} \left[\frac{t_1 + t_2}{2} r^2 - r^3 \right] dr \right\} \tag{A3.6}$$

Integrating and collecting terms yields

$$\overline{\Delta\rho_t^2} = \frac{A_t}{6(\bar{R})^2}\left[\left(\frac{t_1 + t_2}{2}\right)^4 - \left(\frac{t_2 - t_1}{2}\right)^4\right] \tag{A4.6}$$

$$= \frac{A_t}{12(\bar{R})^2}\left(t_2 t_1^3 + t_2^3 t_1\right) \tag{A5.6}$$

$$= \frac{t_1^2 + t_2^2}{12(\bar{R})^2} \quad . \tag{A6.6}$$